First β-decay spectroscopy of ^{135}In and new β-decay branches of ^{134}In

M. Piersa-Siłkowska,[1,*] A. Korgul,[1,†] J. Benito,[2] L. M. Fraile,[2,3] E. Adamska,[1] A. N. Andreyev,[4] R. Álvarez-Rodríguez,[5] A. E. Barzakh,[6] G. Benzoni,[7] T. Berry,[8] M. J. G. Borge,[3,9] M. Carmona,[2] K. Chrysalidis,[3] J. G. Correia,[3,10] C. Costache,[11] J. G. Cubiss,[3,4] T. Day Goodacre,[3,12] H. De Witte,[13] D. V. Fedorov,[6] V. N. Fedosseev,[3] G. Fernández-Martínez,[14] A. Fijałkowska,[1] H. Fynbo,[15] D. Galaviz,[16] P. Galve,[2] M. García-Díez,[2] P. T. Greenlees,[17,18] R. Grzywacz,[19,20] L. J. Harkness-Brennan,[21] C. Henrich,[22] M. Huyse,[13] P. Ibáñez,[2] A. Illana,[13,23] Z. Janas,[1] K. Johnston,[3] J. Jolie,[24] D. S. Judson,[21] V. Karanyonchev,[24] M. Kicińska-Habior,[1] J. Konki,[17,18] Ł. Koszuk,[1] J. Kurcewicz,[3] I. Lazarus,[25] R. Lică,[3,11] A. López-Montes,[2] H. Mach,[26] M. Madurga,[3,19] I. Marroquín,[9] B. Marsh,[3] M. C. Martínez,[2] C. Mazzocchi,[1] K. Miernik,[1] C. Mihai,[11] N. Mărginean,[11] R. Mărginean,[11] A. Negret,[11] E. Nácher,[27] J. Ojala,[17] B. Olaizola,[28,29,3] R. D. Page,[21] J. Pakarinen,[17] S. Pascu,[11] S. V. Paulauskas,[19] A. Perea,[9] V. Pucknell,[25] P. Rahkila,[17,18] C. Raison,[4] E. Rapisarda,[3] K. Rezynkina,[13] F. Rotaru,[11] S. Rothe,[3] K. P. Rykaczewski,[20] J.-M. Régis,[24] K. Schomacker,[24] M. Siłkowski,[1] G. Simpson,[30] C. Sotty,[11,13] L. Stan,[11] M. Stănoiu,[11] M. Stryjczyk,[1,13,17] D. Sánchez-Parcerisa,[2] V. Sánchez-Tembleque,[2] O. Tengblad,[9] A. Turturică,[11] J. M. Udías,[2] P. Van Duppen,[13] V. Vedia,[2] A. Villa,[2] S. Viñals,[9] R. Wadsworth,[4] W. B. Walters,[31] N. Warr,[24] and S. G. Wilkins[3]

(IDS Collaboration)

[1]*Faculty of Physics, University of Warsaw, PL 02-093 Warsaw, Poland*
[2]*Grupo de Física Nuclear and IPARCOS, Universidad Complutense de Madrid, CEI Moncloa, E-28040 Madrid, Spain*
[3]*CERN, CH-1211 Geneva 23, Switzerland*
[4]*Department of Physics, University of York, York, YO10 5DD, United Kingdom*
[5]*Escuela Tecnica Superior de Arquitectura, Universidad Politécnica de Madrid, E-28040 Madrid, Spain*
[6]*Petersburg Nuclear Physics Institute, NRC Kurchatov Institute, 188300 Gatchina, Russia*
[7]*Istituto Nazionale di Fisica Nucleare, Sezione di Milano, I-20133 Milano, Italy*
[8]*Department of Physics, University of Surrey, Guildford GU2 7XH, United Kingdom*
[9]*Instituto de Estructura de la Materia, CSIC, E-28006 Madrid, Spain*
[10]*C2TN, Centro de Ciências e Tecnologias Nucleares, Instituto Superior Técnico, Universidade de Lisboa, Portugal*
[11]*"Horia Hulubei" National Institute of Physics and Nuclear Engineering, RO-077125 Bucharest, Romania*
[12]*School of Physics and Astronomy, The University of Manchester, Manchester M13 9PL, United Kingdom*
[13]*KU Leuven, Instituut voor Kern- en Stralingsfysica, Celestijnenlaan 200D, 3001 Leuven, Belgium*
[14]*Institut für Kernphysik, Technische Universität zu Darmstadt, 64289 Darmstadt, Germany*
[15]*Department of Physics and Astronomy, Aarhus University, DK-8000 Aarhus C, Denmark*
[16]*LIP, and Faculty of Sciences, University of Lisbon, 1000-149 Lisbon, Portugal*
[17]*University of Jyväskylä, Department of Physics, P.O. Box 35, FI-40014, Jyväskylä, Finland*
[18]*Helsinki Institute of Physics, University of Helsinki, FIN-00014 Helsinki, Finland*
[19]*Department of Physics and Astronomy, University of Tennessee, Knoxville, Tennessee 37996, USA*
[20]*Physics Division, Oak Ridge National Laboratory, Oak Ridge, Tennessee 37831, USA*
[21]*Oliver Lodge Laboratory, The University of Liverpool, Liverpool, L69 7ZE, United Kingdom*
[22]*Institut für Kernphysik, Technische Universität Darmstadt, 64289 Darmstadt, Germany*
[23]*Instituto Nazionale di Fisica Nucleare, Laboratori Nazionali di Legnaro, I-35020 Legnaro, Italy*
[24]*Institut für Kernphysik, Universität zu Köln, 50937 Köln, Germany*
[25]*STFC Daresbury, Daresbury, Warrington WA4 4AD, United Kingdom*
[26]*National Centre for Nuclear Research, BP1, PL 00-681 Warsaw, Poland*
[27]*Instituto de Física Corpuscular, CSIC-Universidad de Valencia, E-46071 Valencia, Spain*
[28]*Department of Physics, University of Guelph, Guelph, Ontario, Canada N1G 2W1*
[29]*TRIUMF, 4004 Wesbrook Mall, Vancouver, British Columbia V6T 2A3, Canada*
[30]*Laboratoire de Physique Subatomique et de Cosmologie, IN2P3-CNRS/Université Grenoble Alpes, Grenoble Cedex F-38026, France*
[31]*Department of Chemistry, University of Maryland, Maryland 20742, USA*

(Received 20 July 2021; accepted 28 September 2021; published 26 October 2021)

*Corresponding author: monika.piersa@cern.ch
†agnieszka.korgul@fuw.edu.pl

The β decay of the neutron-rich ^{134}In and ^{135}In was investigated experimentally in order to provide new insights into the nuclear structure of the tin isotopes with magic proton number $Z = 50$ above the $N = 82$ shell. The β-delayed γ-ray spectroscopy measurement was performed at the ISOLDE facility at CERN, where indium isotopes were selectively laser-ionized and on-line mass separated. Three β-decay branches of ^{134}In were established, two of which were observed for the first time. Population of neutron-unbound states decaying via γ rays was identified in the two daughter nuclei of ^{134}In, ^{134}Sn and ^{133}Sn, at excitation energies exceeding the neutron separation energy by 1 MeV. The β-delayed one- and two-neutron emission branching ratios of ^{134}In were determined and compared with theoretical calculations. The β-delayed one-neutron decay was observed to be dominant β-decay branch of ^{134}In even though the Gamow-Teller resonance is located substantially above the two-neutron separation energy of ^{134}Sn. Transitions following the β decay of ^{135}In are reported for the first time, including γ rays tentatively attributed to ^{135}Sn. In total, six new levels were identified in ^{134}Sn on the basis of the $\beta\gamma\gamma$ coincidences observed in the ^{134}In and ^{135}In β decays. A transition that might be a candidate for deexciting the missing neutron single-particle $13/2^+$ state in ^{133}Sn was observed in both β decays and its assignment is discussed. Experimental level schemes of ^{134}Sn and ^{135}Sn are compared with shell-model predictions. Using the fast timing technique, half-lives of the 2^+, 4^+, and 6^+ levels in ^{134}Sn were determined. From the lifetime of the 4^+ state measured for the first time, an unexpectedly large $B(E2; 4^+ \rightarrow 2^+)$ transition strength was deduced, which is not reproduced by the shell-model calculations.

DOI: 10.1103/PhysRevC.104.044328

I. INTRODUCTION

The region around ^{132}Sn, the heaviest doubly magic nucleus far from the valley of β stability, is of great relevance for the development of the theoretical description of neutron-rich nuclei. New experimental data for nuclei in that region allow for a better understanding of phenomena that occur when the N/Z ratio becomes large, such as evolution of shell structure [1–4] and rare processes of β-delayed multiple-neutron emission [5–8]. Properties of nuclei around ^{132}Sn are also important for modeling the rapid neutron capture nucleosynthesis process (r process), since the $A \approx 130$ peak in the r-process abundance pattern is linked to the $N = 82$ shell closure [9–12].

Due to the robust nature of the ^{132}Sn core [13], tin isotopes above $N = 82$ offer a rare opportunity to investigate neutron-neutron components of effective nucleon-nucleon interactions for heavy-mass nuclei with large neutron excess [14]. At present, the ^{132}Sn region is a unique part of the chart of nuclides where spectroscopic information for neutron-rich nuclei with one and few neutrons beyond the double-shell closure was obtained [14–16]. The ^{133}Sn nucleus, with only one neutron outside the doubly magic ^{132}Sn, is the heaviest odd-A tin isotope for which excited states were reported so far [13,15,17–22]. This nuclide has been extensively studied for over two decades to gain information about neutron (ν) single-particle (s. p.) states just outside the closed shell at $N = 82$. Still, the energy of the $\nu 1i_{13/2}$ s. p. state in ^{133}Sn remains unknown. Recently, states having dominant two-particle one-hole (2p1h) neutron configurations with respect to the ^{132}Sn core were identified in ^{133}Sn [20,22]. In the case of even-A tin isotopes above $N = 82$, information on excited states was obtained for ^{134}Sn, ^{136}Sn, and ^{138}Sn [14,16,23,24]. All members of the two-neutron $\nu 2f_{7/2}$ ($\nu 2f_{7/2}^2$) multiplet were reported in these isotopes. An additional state belonging to the $\nu 2f_{7/2} 1h_{9/2}$ configuration is known in ^{134}Sn [23]. Despite extensive studies, information on tin isotopes beyond $N = 82$ still appears to be scarce.

In the present work, we report on the results of a β-decay study of ^{134}In and ^{135}In nuclei that provide new experimental insights into tin isotopes above $N = 82$. In an r-process sensitivity study, ^{134}In and ^{135}In were indicated to be among those β-delayed neutron (βn) emitters that have the greatest impact on the abundance pattern in cold wind r-process simulations [25]. Moreover, for neutron densities around 10^{25} cm^{-3}, where the r-matter flow has already broken through the $N = 82$ shell, the ^{135}In nuclide acts as an important waiting point [26].

The neutron-rich isotopes ^{134}In and ^{135}In represent rare cases of experimentally accessible nuclei for which the β-delayed three-neutron ($\beta 3n$) decay is energetically allowed [6,27]. Therefore, these isotopes are representative nuclei to investigate competition between β-delayed one- ($\beta 1n$) and multiple-neutron ($\beta 2n$, $\beta 3n$, ...) emission as well as the γ-ray contribution to the decay of neutron-unbound states [28,29]. Recently, a significant γ-ray branch for levels above the neutron separation energy S_n was observed in ^{133}Sn [20,22]. As reported in Ref. [20], the main factor that hinders the neutron emission from highly excited 2p1h states in ^{133}Sn is the small overlap of the wave functions of the states involved in the βn decay. It is expected that similar nuclear structure effects play a role for other nuclei southeast of ^{132}Sn, including ^{134}In and ^{135}In [20].

So far, the β decay of ^{134}In was investigated via β-delayed γ-ray spectroscopy in only one measurement, which provided the first information about neutron s. p. states in ^{133}Sn [15,17]. The population of excited states in other tin isotopes was not observed. The βn emission probability P_n was estimated to be around 65% and a β-decay half-life of 138(8) ms was reported for ^{134}In [6,15]. Later, the measurement of β-delayed neutrons from ^{134}In yielded the more precise value of 141(5) ms [26]. Recently, a half-life of 126(7) ms was obtained at RIKEN for ^{134}In [30]. In the case of the ^{135}In β decay, no information on the population of states in tin isotopes existed prior to this work. The β-decay half-life of ^{135}In was measured in two experiments, which yielded values of 92(10) ms [26] and 103(5) ms [30], respectively.

In this work, we observed for the first time the β-decay ($\beta\gamma$) and $\beta 2n$-decay branches of ^{134}In. Transitions following the ^{135}In β decay, including those belonging to the $\beta\gamma$-, $\beta 1n$- and $\beta 2n$-decay branches, were also established for the first time.

II. EXPERIMENTAL DETAILS

The ^{134}In and ^{135}In nuclei were produced at the ISOLDE-CERN facility [31]. The 1.4-GeV proton beam from the Proton Synchrotron Booster (PSB) was directed onto a solid tungsten proton-to-neutron converter [32], producing spallation neutrons that induced fission in a thick uranium carbide target. The indium atoms diffused out of the target material and subsequently effused via a transfer line into the hot cavity ion source, where they were selectively ionized by the Resonance Ionization Laser Ion Source (RILIS) [33]. After extraction and acceleration by a 40 kV potential, the indium isotopes were separated according to the mass-to-charge ratio by the General Purpose Separator and then transmitted to the ISOLDE Decay Station (IDS) [34]. They were implanted on an aluminized mylar tape at the center of the detection setup. The time structure of ions reaching IDS varied depending on the composition of a repetitive sequence of proton pulses, called the supercycle, distributed by the PSB at intervals of 1.2 s. The supercycle structure varied during the experiment and its length ranged from 26 to 34 proton pulses, corresponding to 31.2 and 40.8 s, respectively. The extraction of the ion beam was started 5 ms after each proton pulse from PSB and lasted 500 ms for ^{134}In and 225 ms for ^{135}In.

Data were collected during the beam implantation and the subsequent decay of the isotopes of interest. To suppress the long-lived activity from the decay of daughter nuclei, the tape was moved after each supercycle. Additional measurements were performed with the ^{134}In beam in which the tape was moved after each proton pulse. Surface-ionized isobaric contaminants, ^{134}Cs and ^{135}Cs, were present in the $A = 134$ and $A = 135$ ion beams, respectively. In the case of the $A = 135$ measurements, the isomeric state of ^{135}Cs was a severe source of background. For identification of beam impurities, an additional measurement was performed at mass $A = 135$ with one of the RILIS lasers turned off. In such laser-off mode, only surface-ionized elements reached the IDS, while in the laser-on mode, RILIS-ionized indium was additionally present in the beam.

To detect β particles, a fast-response 3-mm-thick NE111A plastic scintillator was used. It was positioned directly behind the ion collection point and provided a detection efficiency of around 20%. For the γ-ray detection, four high-purity germanium (HPGe) Clover-type detectors and two truncated cone-shaped $LaBr_3$(Ce) crystals [35] coupled to fast photomultiplier tubes (PMTs) were utilized. The PMT anode signals from fast-response detectors were processed by analog constant fraction discriminators and then sent to time-to-amplitude converters (TACs), which provided the time difference between coincident signals from plastic and $LaBr_3$(Ce) detectors. With this configuration, it was possible to perform lifetime measurements for excited states using the advanced time-delayed $\beta\gamma\gamma(t)$ (fast timing) technique [36–38].

The Nutaq digital data-acquisition system [39] was used to record and sample energy signals from all detectors along with outputs from TACs and the reference signal from the PSB. Data were collected in a triggerless mode. Events were reconstructed in the offline analysis, in which they were correlated with the occurrence of the proton pulse.

Energy and efficiency calibrations of γ-ray detectors were performed using ^{152}Eu, ^{140}Ba - ^{140}La, and ^{133}Ba radioactive sources as well as ^{88}Rb and ^{138}Cs samples produced online. High-energy γ rays originating from the background induced by neutrons from the target area were used to extend the energy calibration of HPGe detectors up to 7.6 MeV. The γ-ray photopeak efficiency of the HPGe detectors reached 4% at 1173 keV after the add-back procedure. For each $LaBr_3$(Ce) detector, an efficiency of around 1% at 1 MeV was obtained. Time-response calibrations of $LaBr_3$(Ce) detectors for full-energy peaks as a function of γ-ray energy as well as corrections due to Compton events were included in the fast-timing analysis. More details on the lifetime measurements using the same experimental setup are provided in Refs. [38,40–42].

III. RESULTS

A. β decay of ^{134}In

Transitions following the β decay of ^{134}In were identified by comparing β-gated γ-ray spectra sorted using various conditions on the time of the event with respect to the proton pulse. Lines that can be attributed to γ rays in daughter nuclei are enhanced when this time window is limited to a few hundred milliseconds. Figure 1 shows the β-gated γ-ray spectrum obtained at $A = 134$ during the first 400 ms following the proton pulse. Long-lived background, originating from decays of daughter nuclei and the surface-ionized ^{134m}Cs contaminant, was subtracted from the data presented. Apart from γ rays that can be assigned to the ^{134}In β decay, neutron-induced background arising from inelastic scattering of fast neutrons [44–48], which were emitted from ^{134}In as β-delayed particles, is also prominent.

The three most intense lines in the spectrum shown in Fig. 1, at energies of 854, 1561, and 2004 keV were observed in the previous β-decay study of ^{134}In [15,17]. They were assigned to the ^{133}Sn nucleus as transitions depopulating the $3/2^-$, $(9/2^-)$, and $5/2^-$ states, respectively. These assignments were confirmed later in one-neutron transfer reactions [13,18,19]. The most intense transition at 1561 keV was used to determine the β-decay half-life of ^{134}In. From the time distribution relative to the proton pulse, shown in Fig. 2, the half-life was deduced to be 118(6) ms. This value is consistent with the ^{134}In half-life measured recently at RIKEN, 126(7) ms [30] and slightly differs from the values previously reported in Ref. [15], 138(8) ms, and in Ref. [26], 141(5) ms.

In the present work, the $\beta 1n$-decay branch of ^{134}In is expanded with three transitions, all of which depopulate states above S_n in ^{133}Sn, 2398.7(27) keV [27]. The peak visible in

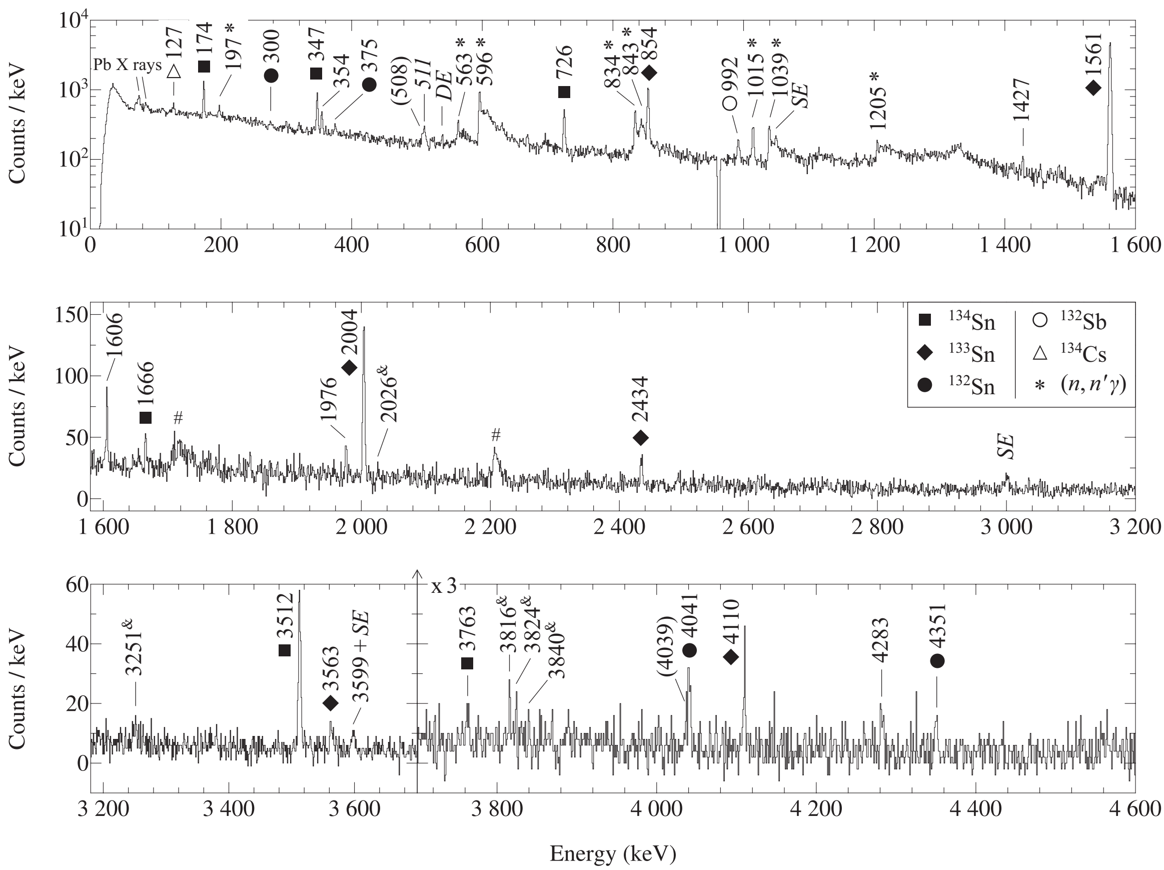

FIG. 1. The β-gated γ-ray spectrum obtained at $A = 134$ in the first 400 ms relative to the proton pulse from which long-lived background has been subtracted. Transitions assigned to the daughter nuclei of ^{134}In are labeled with filled symbols, while those attributed to activities of daughter or contaminant nuclei are marked with open symbols. Transitions that can be assigned to the ^{134}In β decay but not to a specific decay branch are indicated by energy only. Lines marked with an ampersand indicate possible weak transitions whose identification is uncertain. Energies of possible peaks, which might correspond to artifacts due to the background-subtraction procedure, are given in parentheses. The presence of a negative peak at 962 keV is the consequence of subtracting the contribution from the daughter nucleus ^{133}Sn [43]. Triangular-shaped peaks arising from inelastic neutron scattering in the HPGe detectors [44–48] are indicated with asterisks. The peak at 197 keV is also considered as induced by neutrons [46]. The abbreviations *SE* and *DE* indicate single-escape and double-escape peaks, respectively. Broad peaks marked with a hash symbol remain unidentified.

Fig. 1 at 3563 keV corresponds to the transition depopulating the $(11/2^-)$ state in ^{133}Sn. A 3570(50)-keV γ ray was first identified in ^{133}Sn via one-neutron knockout from ^{134}Sn [20]. This was confirmed in a β-decay study of ^{133}In that provided improved precision of its energy, 3563.9(5) keV [22]. The peak visible in Fig. 1 at 4110 keV can be associated with the 4110.8(3)-keV γ ray, which was seen previously in the β decay of ^{133}In [40], but the absence of $\beta\gamma\gamma$ coincidence relations hindered its assignment to a particular daughter nucleus. An observation of this line in the β decays of both ^{133}In and ^{134}In provides support for its assignment to the ^{133}Sn nucleus.

In the energy range corresponding to the predicted excitation energy of the $13/2^+$ state in ^{133}Sn, 2511(80) keV [50] or between 2360 and 2600 keV [51], one relatively intense transition was registered at 2434 keV (see Fig. 1). No $\beta\gamma\gamma$ and $\gamma\gamma$ coincidence relationships were observed for this line, making its assignment to either ^{134}Sn or ^{132}Sn unlikely and thus providing an argument for its assignment to ^{133}Sn. The 2792-keV transition, discussed in Ref. [19] as a possible candidate for γ rays depopulating the $13/2^+$ state in ^{133}Sn, was not observed in the β decay of ^{134}In.

Among the known low-lying levels in ^{133}Sn, only the $1/2^-$ state [13,19,22] was not seen in the ^{134}In β decay. The 354-keV transition that was identified in the previous β-decay study of ^{134}In but remained unassigned despite being registered in coincidence with β-delayed neutrons [15,17] was observed in the present study. No $\beta\gamma\gamma$ and $\gamma\gamma$ coincidence relations were found for this transition, making its attribution to any of the daughter nuclei impossible. The 802-keV transition for which a coincidence with neutrons emitted from ^{134}In was also reported in Refs. [15,17] was not present in our spectra.

We now turn to the $\beta\gamma$-decay branch of ^{134}In, leading to the population of states in ^{134}Sn, which was observed for the first time in this work. Figure 1 shows clearly the presence of the 174-, 347- and 726-keV transitions that were assigned to the yrast $6^+ \rightarrow 4^+ \rightarrow 2^+ \rightarrow 0^+_{\mathrm{g.s.}}$ cascade in ^{134}Sn from the ^{248}Cm fission data [16,23]. The 1262-keV γ ray deexciting the (8^+) state in ^{134}Sn [23] was not observed in the ^{134}In β decay.

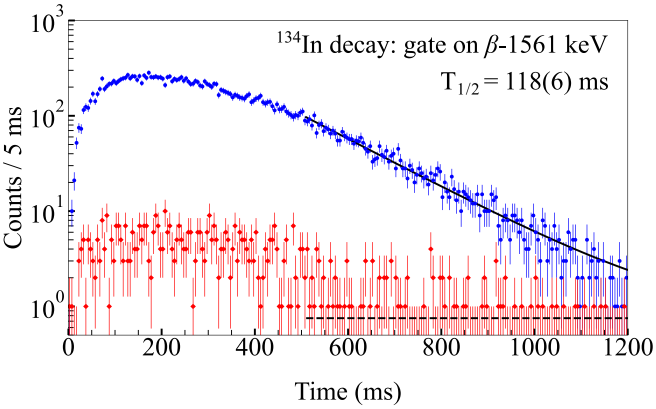

FIG. 2. Time distributions relative to the proton pulse of the 1561-keV transition (blue circles) and the background area (red diamonds) observed in coincidence with β particles at $A = 134$ when RILIS was applied to ionize indium. A function composed of an exponential decay and a constant background was fit (solid line) in the 510–1200 ms time range. The curve corresponding to the background component is also presented (dashed line). A Bayesian approach was applied in the statistical analysis of the data [49].

Analysis of $\beta\gamma\gamma$ coincidences reveals three new transitions in ^{134}Sn. The 1666-, 3512- and 3763-keV lines are seen in spectra of γ rays in coincidence with previously known transitions in this nucleus. Figures 3(a)–3(c) displays the γ-ray spectra in coincidence with new transitions assigned to the daughter nucleus produced in the $\beta\gamma$-decay branch of ^{134}In. Two of them depopulate neutron-unbound states at excitation energies exceeding the S_{1n} of ^{134}Sn, 3631(4) keV [27], by more than 1 MeV.

The $\beta2n$-decay branch of ^{134}In, leading to the population of states in ^{132}Sn, was observed for the first time. Transitions depopulating the 2^+, 3^-, 4^+, and 6^+ states in ^{132}Sn [52], with energies of 4041, 4351, 375, and 300 keV, respectively, were identified (see Fig. 1). Coincidence relationships observed for γ rays in the daughter nucleus produced in the $\beta2n$-decay branch of ^{134}In are shown in Fig. 3(d).

Transitions assigned to the $\beta\gamma$-, $\beta1n$-, and $\beta2n$-decay branches of ^{134}In are summarized in Table I. Several additional transitions were observed with a time pattern consistent with the ^{134}In β-decay half-life. However, due to the lack of $\beta\gamma\gamma$ and $\gamma\gamma$ coincidence relationships, they could not be placed in the β-decay scheme of ^{134}In. These transitions are also listed in Table I.

The β-decay scheme of ^{134}In established in the present work is shown in Fig. 4. The previously reported scheme [15] is now complemented by the $\beta\gamma$- and $\beta2n$-decay branches, with thirteen new transitions assigned to this β decay. Neutron-unbound states decaying via γ rays were identified in two daughter nuclei, ^{134}Sn and ^{133}Sn. It should be emphasized that presumably only a partial β-decay scheme is established in this work, since the β-decay energy of ^{134}In is large ($Q_\beta \approx$ 14.5 MeV [27]) and, as we have presented, the contribution of γ ray deexcitation to the decay of neutron-unbound states in ^{134}Sn and ^{133}Sn is significant.

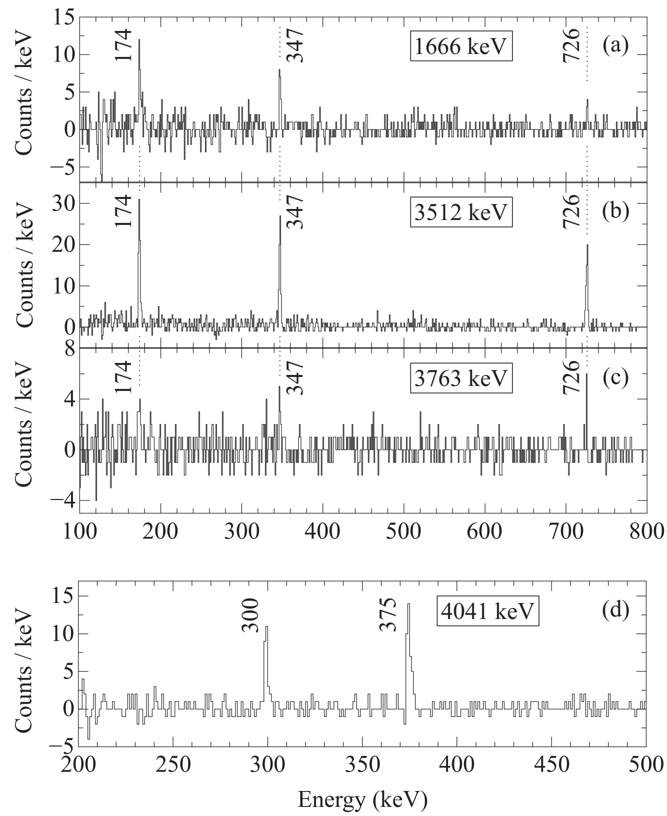

FIG. 3. Background-subtracted γ-ray spectra in coincidence with the (a) 1666-, (b) 3512-, and (c) 3763-keV transitions that depopulate new levels in ^{134}Sn following the $\beta\gamma$ decay of ^{134}In. Vertical dotted lines indicate energies of previously known transitions in ^{134}Sn. (d) Background-subtracted γ-ray spectrum in coincidence with the 4041-keV transition in ^{132}Sn observed in the $\beta2n$ decay of ^{134}In.

Relative intensities of transitions following the ^{134}In β decay were determined from the β-gated γ-ray spectrum. These intensities, normalized to the most intense 1561-keV γ ray, agree with those reported in the previous β-decay study of ^{134}In [15,17]. For the γ rays involved in the 174-347-726 keV cascade decaying from the 6^+ isomeric state in ^{134}Sn, a correction to the intensity extracted from the β-gated γ-ray spectrum due to an isomer half-life of 81.7(12) ns (see Sec. III C) was included. The transition intensities determined from the β-gated γ-ray spectrum as peak areas corrected for efficiency and internal conversion were found to be equal for the 174-, 347-, and 726-keV transitions, suggesting that the 2^+ and 4^+ states in ^{134}Sn are not fed directly in the β decay of ^{134}In within the intensity uncertainties. This is further confirmed by the analysis of the γ-ray spectrum in coincidence with the 347-keV transition, where the ratio of transition intensities for the 174- and 726-keV lines was deduced to be 1.0(1). These observations points to the lack of direct β-decay feeding to the 2^+ and 4^+ states in ^{134}Sn and consequently provides an argument for the high spin value of the ground state of the parent nucleus, which can be 6^- or 7^-.

The probabilities of $\beta1n$ and $\beta2n$ emission from ^{134}In were determined from the ratio of daughter nuclei produced in a

TABLE I. Energies and relative intensities of the transitions observed in the ^{134}In β decay. Total γ-ray and internal-conversion intensities are normalized to the intensity of the 1561-keV transition, for which the absolute intensity is deduced to be 10.8(6)% per β decay of ^{134}In.

Decay branch	Daughter nucleus	Energy (keV)	Relative intensity
$\beta\gamma$	^{134}Sn	173.8(3)	4.9(3)[a]
$\beta\gamma$	^{134}Sn	347.4(3)	4.9(3)[a]
$\beta\gamma$	^{134}Sn	725.6(3)	4.9(4)
$\beta\gamma$	^{134}Sn	1665.5(3)	0.6(1)
$\beta\gamma$	^{134}Sn	3512.3(3)	2.7(3)
$\beta\gamma$	^{134}Sn	3763(1)	0.5(1)
$\beta 1n$	^{133}Sn	854.0(3)	10.4(7)
$\beta 1n$	^{133}Sn	1561.1(3)	100(5)
$\beta 1n$	^{133}Sn	2003.8(3)	3.7(3)
$\beta 1n$[b]	^{133}Sn	2434.2(3)	1.4(2)
$\beta 1n$	^{133}Sn	3563(1)	0.6(2)
$\beta 1n$	^{133}Sn	4110(1)	0.7(2)
$\beta 2n$	^{132}Sn	299.5(3)	0.4(2)
$\beta 2n$	^{132}Sn	375.0(3)	0.48(7)
$\beta 2n$	^{132}Sn	4041.0(5)	0.9(2)
$\beta 2n$	^{132}Sn	4351(1)	0.5(1)
Unassigned:			
Energy (keV)	Relative intensity	Energy (keV)	Relative intensity
354.3(3)	1.5(2)	3599(2)	0.4(1)[c]
1427.4(3)	0.7(2)	3816(1)[d]	<0.4
1605.8(3)	1.0(2)	3824(1)[d]	<0.4
1976.3(3)	0.8(1)	3840(1)[d]	<0.4
2026(1)[d]	<0.5	4283(1)	0.5(1)
3251(1)[d]	<0.4		

[a]Relative intensities were corrected for internal conversion assuming $E2$ character: α_{tot}(174 keV)= 0.227(4) and α_{tot}(347 keV)= 0.0221(4) [53].
[b]See the discussion section for more details on this assignment.
[c]Upper limit, this intensity includes a contribution from the *SE* peak.
[d]The identification is uncertain due to low statistics.

given β-decay branch to the total number of daughter nuclei, using γ rays emitted in their decays. The following transitions and their absolute intensities were used: 872 keV in ^{134}Sb from the ^{134}Sn β decay with 6(3)% [54], 341 keV in ^{132}Sb from the ^{132}Sn β decay with 48.8(12)% [55,56], and 962 keV in ^{133}Sb from the ^{133}Sn β decay with 12(2)% [43]. For the latter, both the β decay of ^{133}Sn and the βn decay of ^{134}Sn contribute to the intensity. For the βn-decay branch of ^{134}Sn we use the 1.4% feeding of the 962-keV state in ^{133}Sb reported in Ref. [54]. The γ-ray intensities obtained from the singles γ-ray spectrum were used to derive the probabilities. Corrections to the recorded activity of daughter nuclei due to tape movement were included based on the reconstructed average supercycle structure. In this way we obtained branching ratios for the β decay of ^{134}In: $P_{0n} = 2.2(15)\%$, $P_{1n} = 89(3)\%$, and $P_{2n} = 9(2)\%$. The P_{1n} value obtained in our estimate is larger than the βn-decay branching ratio evaluated from the previous β-decay study of ^{134}In, $P_n \approx 65\%$ [6,15,57].

B. β decay of ^{135}In

Spectra acquired at $A = 135$ are dominated by the decay of the surface-ionized ^{135}Cs. Figure 5 shows a comparison of the β-gated γ-ray spectra measured in laser-on and laser-off modes. Despite strong isobaric contamination of the RILIS-ionized beam, we were able to identify for the first time transitions following the ^{135}In β decay. The two most intense lines seen only in the spectrum collected when RILIS was used to ionize indium, at 347 and 726 keV, correspond to known γ rays in ^{134}Sn. The β-decay half-life of ^{135}In was determined from the time distributions of the 347- and 726-keV transitions which yielded $T_{1/2} = 89(10)$ ms and 90(9) ms, respectively. The decay curve of the 347-keV γ ray is shown in Fig. 6. The weighted average of 89(7) ms is in agreement with the half-life previously determined at ISOLDE by measuring the β-delayed neutrons, 92(10) ms [26], and slightly lower than the half-life of 103(5) ms measured at RIKEN [30]. Based on the systematics of the lighter odd-A indium isotopes, a β-decaying isomer in ^{135}In is expected to exist, with a half-life similar to the ground state [58]. However, no evidence for its presence was found in this work.

Suppression of the background observed at $A = 135$ became crucial for the identification of other transitions following the ^{135}In β decay. Two approaches were used independently in our analysis to reduce contaminants. One strategy was to apply a gate on the first few hundred milliseconds after the proton pulse and subtract events recorded at delayed intervals, leading to a substantial decrease in contamination from 53(2)-min ^{135m}Cs [59]. The second approach was to study γ rays observed in coincidence with the highest-energy deposit in the plastic detector in order to preferentially select ^{135}In β decay. Figure 7 shows the γ-ray spectra built using two different β-gating conditions. By comparing these spectra, transitions following the ^{135}In β decay were established. Their energies and relative intensities, which were determined from the β-gated γ ray spectrum, are listed in Table II. Figure 8 shows the β-decay scheme of ^{135}In established in this work.

The most intense transitions observed in the ^{135}In β decay belong to ^{134}Sn. Three lines that can be attributed to the previously known γ rays in ^{133}Sn were also identified. The 2434-keV transition, which was seen in the ^{134}In β decay, was also observed in the ^{135}In β decay and is a plausible candidate for a new transition in ^{133}Sn. As for the possible $\beta 3n$-decay branch of ^{135}In, a slight excess of counts over background appears in the γ-ray spectrum around 4041 keV, corresponding to the energy of the first-excited state in ^{132}Sn [40,52]. The low statistics does not allow it to be firmly established whether the $\beta 3n$-decay branch has been observed in this work for ^{135}In.

Using $\beta\gamma\gamma$ coincidence data, new transitions were identified in ^{134}Sn. Figure 9 displays the β-gated γ-ray spectra in coincidence with the 347- and 726-keV transitions that reveal three new γ rays in ^{134}Sn with energies of 857, 1094, and 1405 keV. These transitions were placed in the level scheme of ^{134}Sn as depopulating levels at excitation energies of 1930,

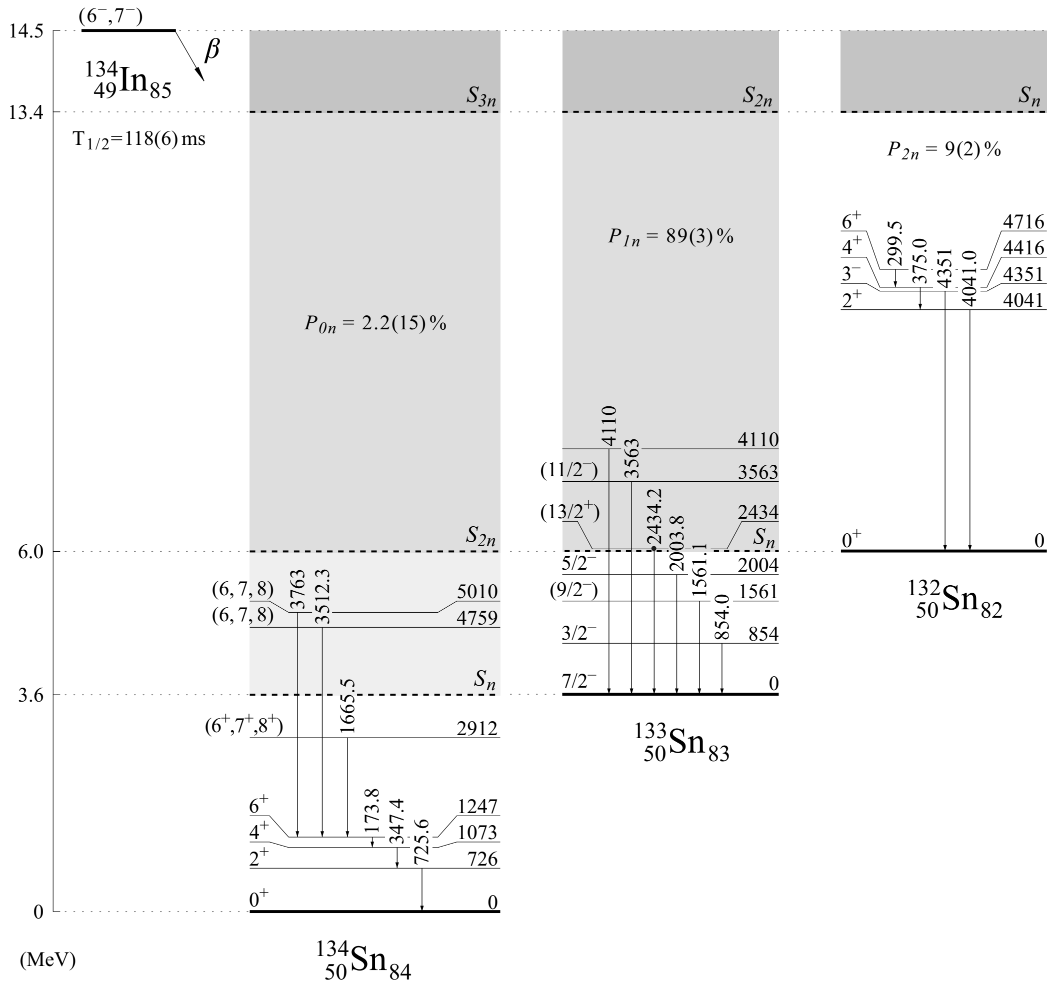

FIG. 4. Decay scheme of ^{134}In established in the present work. Excited states in the daughter nuclei are labeled with energies (in keV) given relative to the ground state of each tin isotope. The spin-parity assignments for previously known states in tin isotopes are taken from Refs. [15,16,20,52]. The ground-state spin and parity of ^{134}In was proposed based on our experimental findings. Shell-model predictions and systematics discussed in Sec. IV A favor the 7^- assignment. The left vertical scale (in MeV) shows the excitation energy and (multi-) neutron separation energies with respect to the ^{134}Sn ground state. The shaded regions represent energy windows for population of (multi-) neutron-unbound states. The Q_β, S_n, S_{2n}, and S_{3n} values are taken from Ref. [27].

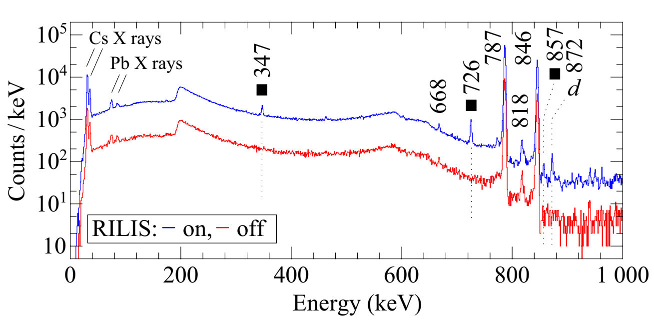

FIG. 5. The β-gated γ-ray spectrum obtained at $A = 135$ when RILIS was applied to ionize indium (upper blue curve) and when one of the RILIS lasers was blocked (lower red curve). Some of the most prominent transitions are labeled with their energies (in keV). Peaks present in both spectra originate from the contaminants, while those appearing only in the RILIS-on mode can be attributed to the β decay of ^{135}In (square) or its daughter nucleus (marked with "d").

2167, and 2478 keV, respectively (see Fig. 8). Tentative assignment to ^{134}Sn was made for the 595-keV transition, which was found in coincidence with that at 726 keV but was not observed in the γ-ray spectra sorted with two different β-gating conditions (see Fig. 7).

Several new lines, which were not observed in the β decays of the lighter indium isotopes, were seen in the ^{135}In β decay. They are listed in Table II. Based on the available experimental information on daughter nuclei produced in the $\beta 1n$- and $\beta 2n$-decay branches of ^{135}In, at least two of them can be considered as transitions in ^{135}Sn. For ^{134}Sn, identification of new levels below the excitation energy of the 6^+ state (at 1247 keV) is unlikely [16,23,24]. For ^{133}Sn, new levels below 2004 keV are also not expected [15,17–22]. Therefore, the 950- and 1221-keV lines, being the most intense in the considered energy range and for which no coincident γ rays were observed, were attributed to deexcitations in ^{135}Sn. Due to the higher excitation energies of other transitions as well

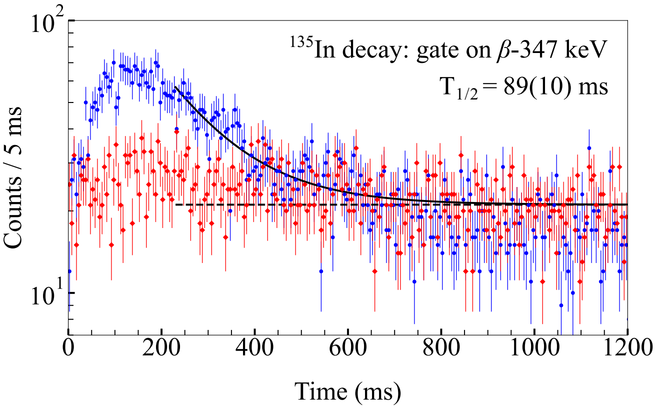

FIG. 6. Time distribution relative to the proton pulse of the 347-keV transition (blue circles) and the background area (red diamonds) observed in coincidence with β particles at $A = 135$ in the laser-on mode. A function composed of an exponential decay and a constant background was fit (solid line) in the 230–1200 ms time range. The curve corresponding to the background component is also presented (dashed line). A Bayesian approach was applied in the statistical analysis of the data [49].

as the lack of $\beta\gamma\gamma$ and $\gamma\gamma$ coincidences for them, it was not possible to attribute them to ^{135}Sn or ^{134}Sn.

Due to the overwhelming long-lived background in the singles and β-gated γ-ray spectra, evaluation of the intensities of γ rays following β decays of tin isotopes was not possible. Thus, absolute intensities of transitions assigned to the ^{135}In β decay could not be determined. Based on relative transition intensities, it can be concluded that the ^{135}In β decay is dominated by the $\beta 1n$ emission.

C. Lifetime measurements for ^{134}Sn

For the three lowest excited states in ^{134}Sn, it was possible to measure their lifetimes using data from both the ^{134}In and ^{135}In β decays. The fast-timing analyses of these two β decays have their own limitations. In the case of ^{134}In, acquiring high statistics for transitions in ^{134}Sn was limited by the large $P_{1n} = 89(3)\%$ and $P_{2n} = 9(2)\%$ values for the parent nucleus. For this reason, it was beneficial to include in the lifetime analysis the data collected for ^{135}In, despite the beam-contamination problems and over an order of magnitude fewer implanted ions of ^{135}In than ^{134}In. The statistics obtained in these two β decays precluded the use

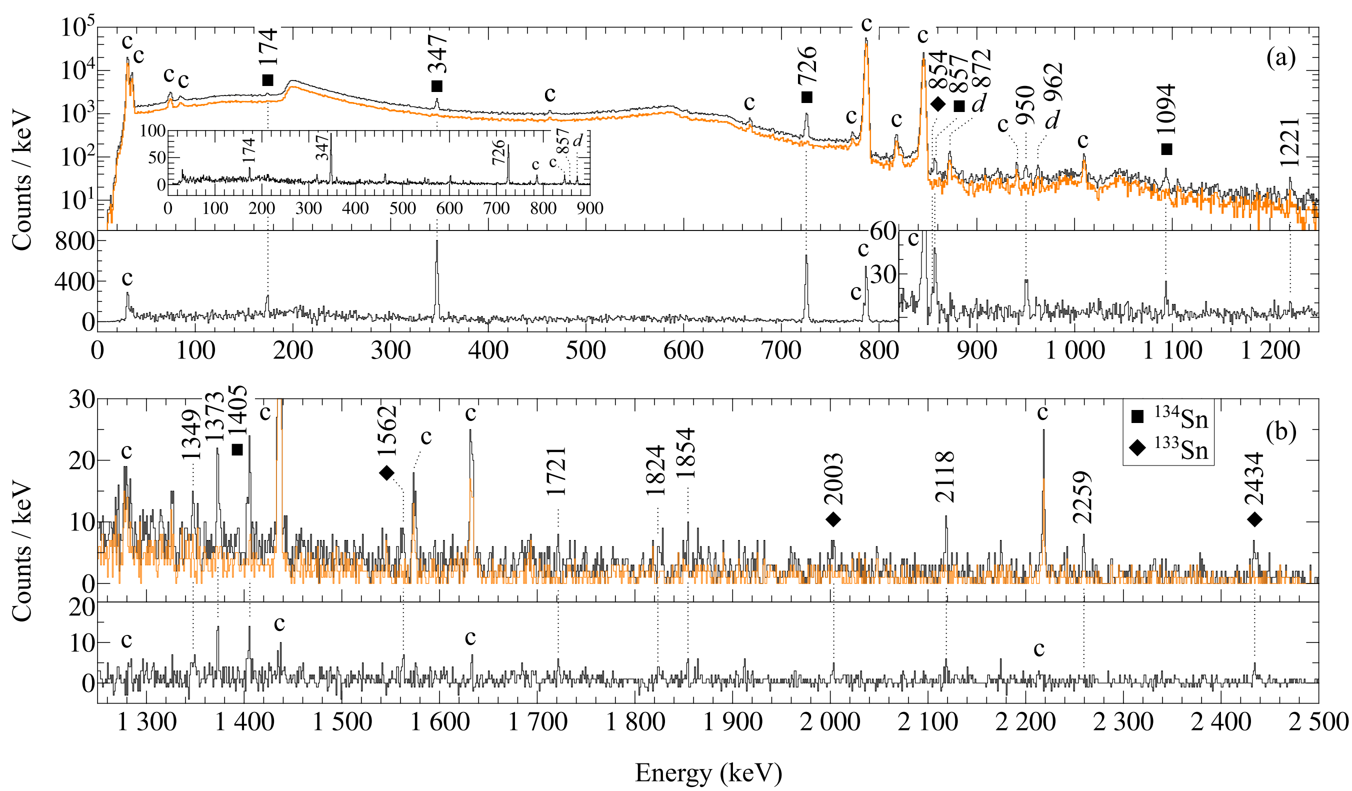

FIG. 7. The β-gated γ-ray spectra obtained at $A = 135$ in the laser-on mode in which different conditions on time with respect to the proton pulse were applied. [(a), (b), top panels] The orange (gray) curve shows the spectrum gated at times later than 600 ms relative to the proton pulse, while the black curve shows the spectrum without any condition imposed on the time of the event with respect to the proton pulse. The inset in panel (a) shows a portion of the spectrum with an increased energy threshold for β particles. [(a), (b), bottom panels] The β-gated γ-ray spectrum recorded in the first 400 ms relative to the proton pulse from which long-lived background was subtracted. Transitions assigned to the $\beta 1n$- and $\beta 2n$-decay branches of ^{135}In are marked with squares and diamonds, respectively. Peaks that can be attributed to γ rays following ^{135}In β decay are indicated by energy only, while those assigned to activities of the daughter or contaminant nuclei are marked with "*d*" and "*c*," respectively.

of triple coincidences $\beta\gamma\gamma(t)$. Nevertheless, by investigating the time response of the background and introducing relevant corrections [38,40], half-lives were determined by using double-coincidence events [42].

The half-life of the 6^+1247-keV state in ^{134}Sn was previously reported as 80(15) ns [16] and, more recently, as 86^{+8}_{-7} ns [24]. Such a long half-life can be measured using the timing information from the HPGe detectors. Figure 10(a) shows the $\beta - \gamma_{\mathrm{HPGe}}(t)$ time distributions gated on the 174-, 347-, and 726-keV transitions forming the $6^+ \rightarrow 4^+ \rightarrow 2^+ \rightarrow 0^+_{\mathrm{g.s.}}$ cascade from which the half-life of the 6^+ level was determined to be 81.7(12) ns. This value is in agreement with those previously reported but has a significantly improved precision. Determination of the lifetime for the 4^+1073-keV level in ^{134}Sn requires the use of fast γ-ray detectors. The $\gamma_{\mathrm{LaBr_3(Ce)}} - \gamma_{\mathrm{LaBr_3(Ce)}}(t)$ coincidences observed in the ^{134}In β decay between two scintillation detectors were used to obtain the time difference between the 174-keV transition feeding the 4^+ state at 1073 keV and the 347-keV transition depopulating it. Figure 10(b) displays the resulting delayed and antidelayed time distributions. In the ^{135}In β decay, the 6^+ isomeric state in ^{134}Sn is weakly populated and the same approach was not possible. In this case, the lifetime was derived by analyzing the $\beta - \gamma_{\mathrm{LaBr_3(Ce)}}(t)$ time distributions gated on the 347- and 726-keV γ rays depopulating the 4^+ and 2^+ states in ^{134}Sn, respectively. By combining the results from both β decays, the half-life of the 4^+ state in ^{134}Sn was measured for the first time and determined to be 1183(40) ps.

For the 2^+726-keV state in ^{134}Sn, the lifetime has not been directly measured to date. A half-life of 49(7) ps was deduced from $B(E2; 0^+ \rightarrow 2^+) = 0.029(5)$ $e^2\,\mathrm{b}^2$ obtained in a Coulomb excitation measurement [60]. To extract the half-life of the 2^+ state, the $\gamma_{\mathrm{LaBr_3(Ce)}} - \gamma_{\mathrm{LaBr_3(Ce)}}(t)$ coincidences between the 347- and 726-keV γ rays were analyzed. Due to the limited statistics, this was only feasible using the ^{134}In β-decay data. The determined centroid positions suffered from low statistics. Figure 10(c) shows the time distributions for the 347–726 keV delayed and antidelayed coincidences from which a half-life of 53(30) ps was determined for the 2^+ state. This value is consistent with the one deduced from the Coulomb excitation measurement [60].

TABLE II. Energies and relative intensities of transitions observed in the ^{135}In β decay. Total γ-ray and internal-conversion intensities are normalized to the intensity of the 726-keV transition.

Decay branch	Daughter nucleus	Energy (keV)	Relative intensity
$\beta\gamma$[a]	^{135}Sn	950.3(3)	7(1)
$\beta\gamma$[a]	^{135}Sn	1220.9(3)	4.0(9)
$\beta 1n$	^{134}Sn	173.8(3)	25(5)[b]
$\beta 1n$	^{134}Sn	347.4(3)	74(5)[b]
$\beta 1n$[a]	^{134}Sn	595(1)[c]	11(5)[d]
$\beta 1n$	^{134}Sn	725.6(3)	100(6)
$\beta 1n$	^{134}Sn	857.2(3)	7(1)
$\beta 1n$	^{134}Sn	1093.8(6)	6(1)
$\beta 1n$	^{134}Sn	1404.8(6)	3.9(8)
$\beta 2n$	^{133}Sn	854.0(8)	1.6(9)
$\beta 2n$	^{133}Sn	1562.4(8)	2.0(6)
$\beta 2n$	^{133}Sn	2003.3(8)	1.8(6)
$\beta 2n$[e]	^{133}Sn	2434.2(7)	2.6(7)
Unassigned:			
Energy (keV)	Relative intensity	Energy (keV)	Relative intensity
1349.2(9)	2.4(7)	1853.1(8)	2.2(7)
1372.9(3)	3.3(8)	2118.3(6)	2.5(7)
1720.9(8)	1.2(5)	2259.3(8)	1.8(6)
1824.0(8)	2.0(7)	2516.1(8)	1.5(5)

[a]Tentatively assigned to this β-decay branch of ^{135}In.
[b]Relative intensities were corrected for internal conversion assuming $E2$ character: $\alpha_{\mathrm{tot}}(174\ \mathrm{keV}) = 0.227(4)$ and $\alpha_{\mathrm{tot}}(347\ \mathrm{keV}) = 0.0221(4)$ [53].
[c]Transition observed only in $\beta\gamma\gamma$ coincidence.
[d]Intensity obtained from coincidences.
[e]See the discussion section for more details on this assignment.

IV. DISCUSSION

A. β decay of ^{134}In

The ground-state configuration of ^{134}In, with $Z = 49$ and $N = 85$, is based on the coupling of the proton hole in the $\pi 1g_{9/2}$ orbital and three neutrons in the $\nu 2f_{7/2}$ orbital (see Fig. 11).

The ^{134}In ground-state spin and parity have not been determined experimentally yet. However, in the previous β-decay study of ^{134}In, it was possible to restrict the expected spin-parity values to a range from 4^- to 7^-, with 7^- being favored, based on the observed β-decay feeding to excited states in ^{133}Sn and on systematics [15]. The observation of the β-decay feeding to only one member of the $\nu 2f^2_{7/2}$ multiplet in ^{134}Sn, the one with maximum spin value of 6^+, is another argument for a high ground-state spin of the parent nucleus, which can be 6^- or 7^-. For the analogous configuration $\pi 1g^{-1}_{9/2}\nu 2f_{7/2}$ in ^{132}In, the 7^- state is the lowest-lying member of the multiplet [52,62]. Thus, the 7^- ground state can also be expected in ^{134}In. This ground-state spin-parity assignment is supported by shell-model calculations that reproduce the recently identified 3.5(4)-μs isomer in ^{134}In decaying by an $E2$ transition [63]. Shell-model calculations with two different interactions consistently predict 7^- as the ^{134}In ground state, while the 6^- state is expected to lie above the 5^- isomer [63]. Therefore, we consider 7^- as the most likely ground-state spin-parity assignment for ^{134}In.

The β decay of ^{134}In is dominated by the Gamow-Teller (GT) $\nu 1g_{7/2} \rightarrow \pi 1g_{9/2}$ transition [64]. Since this GT decay involves deeply bound neutrons in the $N = 82$ ^{132}Sn core, it populates neutron-unbound states in the daughter nucleus (see Fig. 11). These are expected in ^{134}Sn at excitation energies comparable to the energy of the 6^- state in ^{132}Sn (7211 keV), arising from the $\nu 1g^{-1}_{7/2}2f_{7/2}$ configuration, which is populated in the GT decays of ^{132}In [40,52]. This implies that the prevalent β-decay feeding is located well above the S_{2n} of ^{134}Sn, 6030(4) keV [27]. As a result, the ^{134}In β decay proceeds mainly through βn-emission branches. The observed

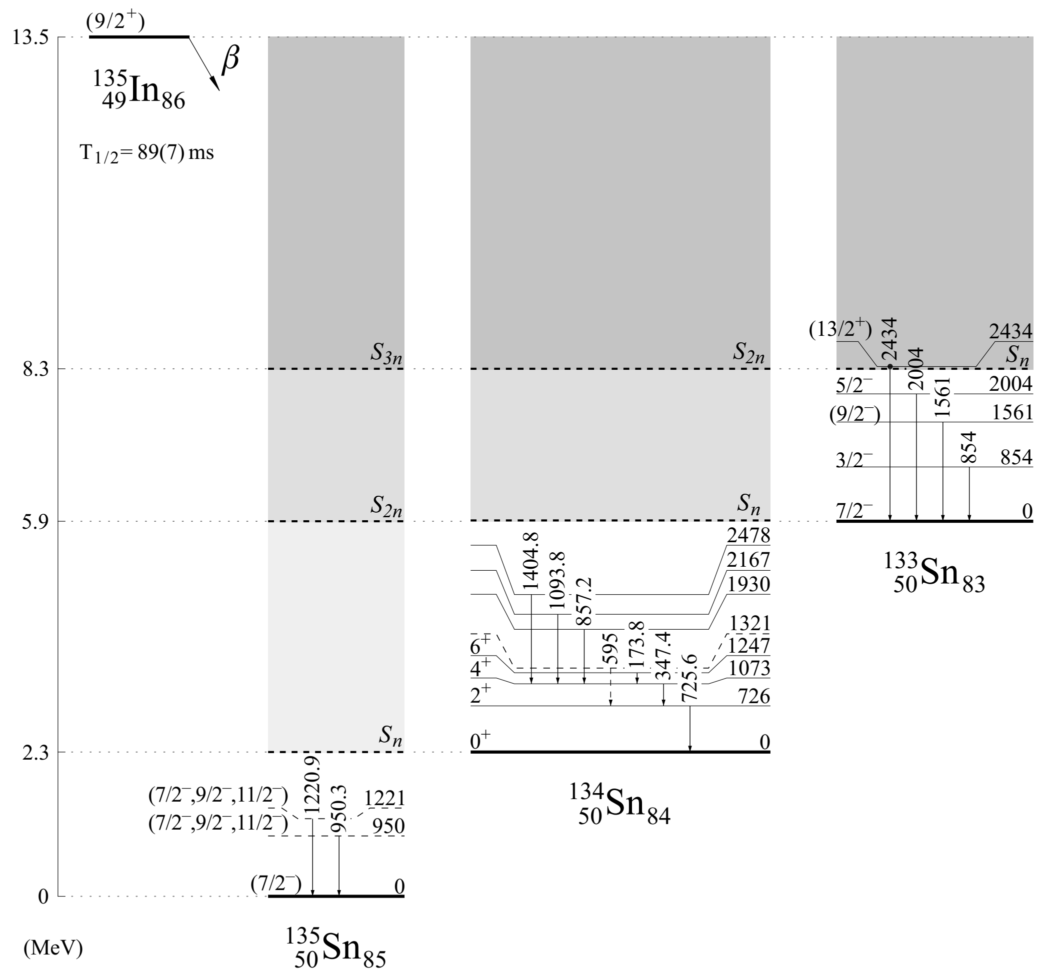

FIG. 8. Decay scheme of ^{135}In established in this work. Excited states in daughter nuclei are labeled with energies (in keV) given relative to the ground state of each tin isotope. Levels tentatively proposed in ^{135}Sn and ^{134}Sn are indicated with dashed lines. The spin-parity assignments for previously known states in ^{134}Sn and ^{133}Sn are taken from Refs. [15,16]. The ground-state spin and parity of ^{135}Sn and ^{135}In are based on systematics [59]. The left vertical scale (in MeV) shows the excitation energy and (multi-) neutron separation energies with respect to the ^{135}Sn ground state. The shaded regions represent energy windows for population of neutron-unbound states. The Q_β, S_n, S_{2n}, and S_{3n} values are taken from Refs. [27].

population of the 6^+4716-keV state in the $\beta 2n$-decay daughter nucleus ^{132}Sn indicates that there is significant β-decay feeding to neutron-unbound states in ^{134}Sn at excitation energies exceeding 10 MeV. This β-decay strength most likely originates from GT transitions involving proton particle-hole excitations across the $Z = 50$ shell gap (see Fig. 11).

The obtained $\beta 1n$- and $\beta 2n$-decay branching ratios for ^{134}In allow for verification of the predictions of the models used for calculating β-delayed particle emission, which are employed in *r*-process nucleosynthesis modeling. There are presently only two known $\beta 2n$ emitters in the ^{132}Sn region for which P_{2n} have been measured [6,65]: ^{136}Sb with $P_{2n} = 0.14(3)\%$ [66] and ^{140}Sb with $P_{2n} = 7.6(25)\%$ [67].

The P_{1n} and P_{2n} probabilities obtained in this work are compared with theoretical predictions based on quasiparticle random-phase approximation (QRPA) [68], relativistic Hartree-Bogoliubov (RHB) model with the proton-neutron relativistic QRPA (RQRPA) [7], as well as phenomenological effective density model (EDM) [69] (see Table III). For the QRPA, it is possible to compare three successively extended models, some of which take into account not only GT transitions but also first-forbidden (*ff*) transitions and competition between all available decay branches of neutron-unbound states. The inclusion of *ff* transitions in the QRPA-2 model [70] leads to an increase in the $\beta 1n$-decay branching ratio by a factor of about ten with respect to the previous model, QRPA-1, in which only GT transitions were considered [68]. A larger contribution of the $\beta 1n$ emission from ^{134}In is predicted by RHB + RQRPA [7], which accounts for both GT and *ff* transitions. However, in the RHB + RQRPA calculations, the total probability of βn emission ($P_{n,\mathrm{tot}}$) is lower (≈66%) than in the two first variants of the QRPA calculations, where $P_{n,\mathrm{tot}}$ exceeds 90%. Besides, the predicted branching ratio of the $\beta 1n$ decay remains lower than the experimental result. The dominant contribution of the $\beta 1n$ emission is predicted by the most recent QRPA calculations in which the statistical Hauser-Feshbach (HF) model [28] is incorporated to address competition between γ-ray, one- and multiple-neutron

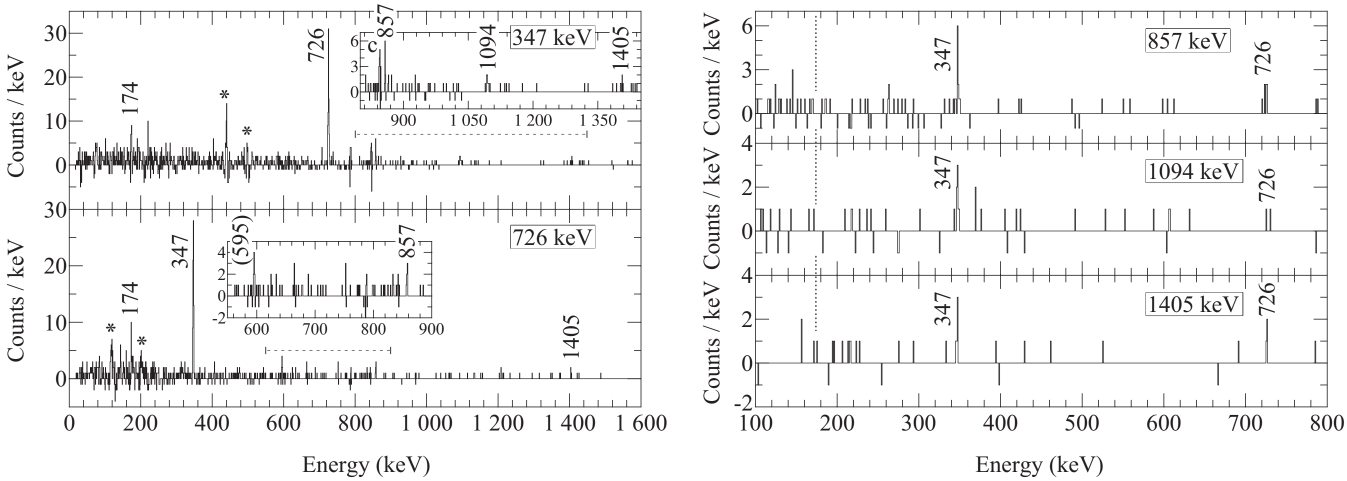

FIG. 9. (left panel) Background-subtracted, β-gated γ-ray spectra in coincidence with the 347- and 726-keV transitions that depopulate previously known levels in ^{134}Sn following the $\beta 1n$ decay of ^{135}In. Peaks that can be attributed to new transitions in ^{134}Sn are labeled with their energies in keV. Tentative assignments are given within brackets. Asterisks indicate artifacts due to the background subtraction procedure. The insets display expanded regions whose ranges are indicated with dashed lines. (right panel) Background-subtracted, β-gated γ-ray spectra in coincidence with newly identified transitions in ^{134}Sn observed in the β decay of ^{135}In.

emission in the decay of neutron-unbound states (QRPA + HF) [71]. The P_{1n} value predicted by the QRPA + HF model, which also accounts for *ff* transitions, is the closest to the experimental value among the models considered. In the case of the P_{2n}, the experimental value is well reproduced only by the EDM. This approach also accounts for the competition between one- and multiple-neutron emission as well as γ-ray emission above S_n. If the cutoff method is applied to the EDM, so that the decay of states above S_{1n} (S_{2n}) proceeds only via emission of one (two) neutron(s), the calculated probabilities change significantly, $P_{1n} = 28\%$ and $P_{2n} = 39\%$ [8].

A comparison of the different $P_{1n,2n}$ calculations shows that the best reproduction of the experimental values for ^{134}In is achieved when *ff* transitions and all possible deexcitation paths of neutron-unbound states are taken into account. Indeed, the inclusion of competition between the emission of one and multiple neutrons as well as γ rays following the ^{134}In β decay is relevant, as in this work the $\beta 1n$-decay branch of ^{134}In was observed to be dominant even though the GT resonance is located substantially above S_{2n} of ^{134}Sn. Moreover, neutron-unbound states decaying via γ rays were observed in the two daughter nuclei, ^{134}Sn and ^{133}Sn. In the one-neutron knockout reaction from ^{134}Sn, it was estimated that around 25%–35% of the decay of neutron-unbound states populated in ^{133}Sn proceeds via γ-ray emission [20]. The enhanced γ-ray emission from states above S_n was explained by the small spectroscopic overlap between states involved in neutron emission.

A similar nuclear structure effect is expected to play a role in the β decay of ^{134}In, both in $\beta\gamma$- and $\beta 1n$-decay branches. The GT decays of neutrons from the $N = 82$ ^{132}Sn core result in population of states in ^{134}Sn formed by couplings of the valence neutrons to core excitations ($\nu^{-1}\nu^3$ or $\pi\pi^{-1}\nu^2$, see Fig. 11). The wave functions of the states populated following neutron emission have small spectroscopic overlaps with the low-lying states in ^{133}Sn, having a single-particle nature [13]. For this reason, γ rays are able to compete with neutron emission well above S_{1n}. Similar structure effects leading to hindrance of neutron emission were identified in other βn emitters [72–74]. The QRPA + HF calculations estimate a minor change, below 3%, in the calculated βn emission probability if an increase of one order of magnitude to the γ-ray strength function is assumed [28]. However, such enhancement of γ-ray emission would have a larger effect on the neutron capture rates of neutron-rich nuclei.

The population of states below the excitation energy of 7 MeV in ^{134}Sn is due to *ff* β decays of ^{134}In. One of these, the $\nu 1h_{11/2} \rightarrow \pi 1g_{9/2}$ transition, which involves neutrons from the $N = 82$ ^{132}Sn core, feeds neutron-unbound states located below the GT resonance (see Fig. 11). The two new states identified in ^{134}Sn at excitation energies around 5 MeV are most likely members of the $\nu 1h^{-1}_{11/2} 2f^3_{7/2}$ multiplet. This assignment is supported by shell-model calculations with core excitations, which predict the first state from this multiplet at around 5 MeV (see Fig. 12) [75]. An analogous $(11/2^-)$ state in ^{133}Sn, resulting from the coupling of a neutron hole in the $\nu 1h_{11/2}$ orbital and two neutrons in the $\nu 2f_{7/2}$ orbital, was identified at 3564 keV [15,20,22]. The 1.26-MeV neutrons [15] and 3564-keV γ rays [22] were assigned to the decay of the $(11/2^-)$ state in ^{133}Sn in β-decay studies of ^{133}In. The observation of a 3563(1)-keV transition in this work implies that this neutron-unbound $(11/2^-)$ state is also populated via the $\beta 1n$ decay of ^{134}In. A certain analogy can be noted to the population pattern observed in the βn decay of ^{132}In, which proceeds primarily through the high-spin $(11/2^-)$ isomer in ^{131}Sn [40,76]. In the β decay of ^{134}In, states with configurations involving neutron hole in the $\nu 1h_{11/2}$ orbital are populated in each observed β-decay branch. These states are neutron-unbound in both ^{134}Sn and ^{133}Sn. However, γ-ray deexcitation has a significant contribution to their decay. This means that states populated following neutron emission, with hole in the $\nu 1h_{11/2}$ orbital, have little overlap with

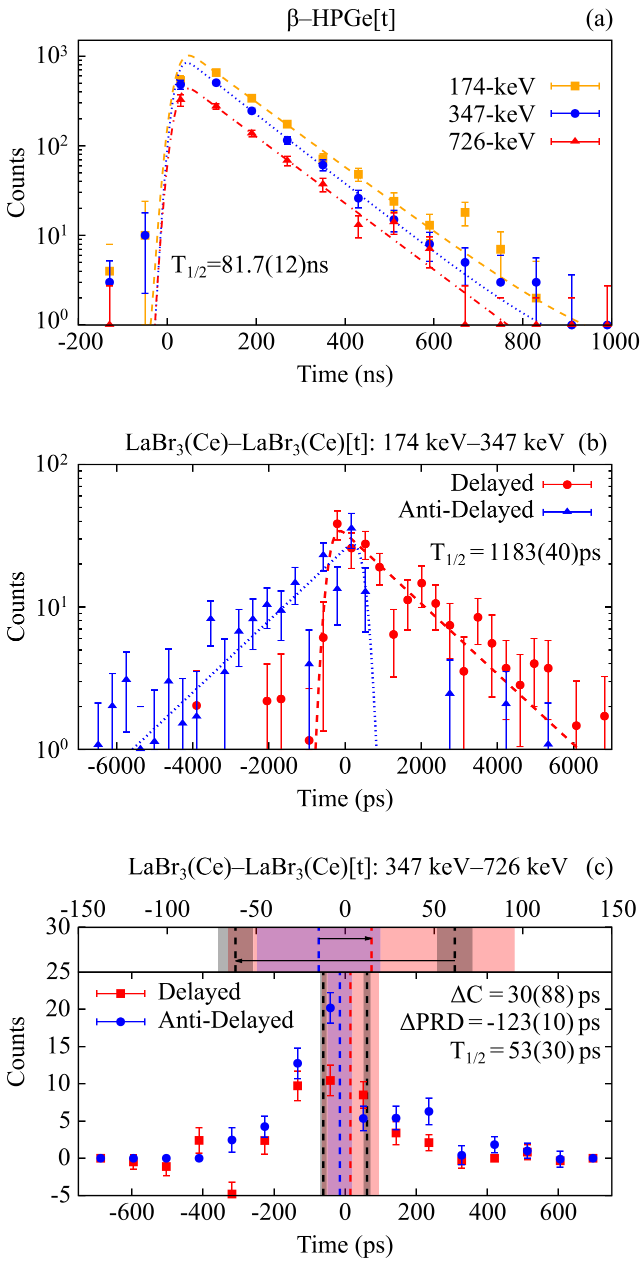

FIG. 10. Time spectra used to measure the lifetimes of the (a) 6^+1247-keV, (b) 4^+1073-keV, and (c) 2^+726-keV states in ^{134}Sn. In panels (a) and (b), the half-life is derived from fit of the slopes, while in panel (c), it is extracted from the centroid-shift measured between the delayed and antidelayed time spectra (ΔC), which is caused by the lifetime of the level and the shift in the Prompt Response Distribution curves (ΔPRD) [38,40,41]. See the text for details.

low-energy states in the corresponding βn-decay daughter nuclei, which correspond to excitations of valence neutrons in the $N = 82$–126 shell.

The large $P_{1n} = 89(3)\%$ value and the expected 7^- ground-state spin and parity for ^{134}In set favorable conditions to search for the missing $\nu 1i_{13/2}$ s. p. state in ^{133}Sn. The high excitation energies of the predicted multiplets in ^{134}Sn involving the $\nu 1i_{13/2}$ orbital are also advantageous. The lowest-lying state arising from the $\nu 2f_{7/2}1i_{13/2}$ configuration is expected at an excitation energy of around 4–5 MeV [77] or 3.2 MeV [78], where negative-parity particle-hole excitations are also expected to appear. Due to the negative parity of states involving the $\nu 1i_{13/2}$ orbital and the expected high density of such levels in ^{134}Sn [78], there is a chance that they are mixed with other neutron-unbound states of negative parity. Such admixtures would increase the overlap of the wave functions of states involved in the $\beta 1n$ decay in which the $13/2^+$ state in ^{133}Sn can be populated. Since there is a wide range of spins, from $3/2^-$ to $(11/2^-)$, for the states populated in ^{133}Sn following the ^{134}In β decay, the population of the $13/2^+$ state does not seem to be hindered in terms of the angular momentum for neutron emission.

The excitation energy of the first $13/2^+$ level in ^{133}Sn was estimated to be 2511(80) keV [50] or between 2360 and 2600 keV [51]. The 2434-keV transition, which is the only one registered in the energy range from 2100 to 3500 keV that can be attributed to the β decay of ^{134}In (see Fig. 1), is therefore a natural candidate for a transition deexciting the $13/2^+$ state in ^{133}Sn. Due to the large difference between the ^{134}In and ^{134}Sn ground-state spins, direct or indirect feeding of an excited state in ^{134}Sn that decays to the 0^+ ground state is unlikely in the ^{134}In β decay. The 2434-keV transition is also observed in the ^{135}In β decay, in which other states in ^{133}Sn are populated in the $\beta 2n$-decay branch.

The decay of the $13/2^+$ state to the $7/2^-$ ground state in ^{133}Sn can proceed via an $E3$ transition with an expected lifetime of around 2 ns. In the analogous nucleus in the ^{208}Pb region with one neutron above the core, ^{209}Pb, a $15/2^-$ level corresponding to the $\nu 1j_{15/2}$ s. p. state decays via an $E3$ transition to the $9/2^+$ ground state ($\nu 2g_{9/2}$) and via an $M2$ transition to the $11/2^+$ excited state ($\nu 1i_{11/2}$) [79,80]. The observed relative intensities of these two transitions are 100(2) and 11(1), respectively. Relying on the similarity of the corresponding excitations in the ^{132}Sn and ^{208}Pb regions [43,50,81–84], the $E3$ transition is anticipated to dominate the decay of the $13/2^+$ state in ^{133}Sn. It is worth mentioning that a transition with energy of 2434 keV was identified in ^{131}Sn [85]. However, an excited state with that energy cannot be populated in ^{131}Sn following the ^{134}In β decay due to an insufficient β-decay energy window.

For the three newly identified states in ^{134}Sn, populated by the ^{134}In β decay, it is possible to propose their spins taking into account the observed γ-ray depopulation pattern and the favored 7^- ground-state spin-parity assignment for the parent nucleus. Spin values for the 2912-, 4759-, and 5010-keV levels can be limited to a range from 6 to 8, since their decay to the 6^+ state at 1247 keV was observed, while the γ-ray decay branch to the 4^+ level at 1073 keV was not identified. For the state at 2912 keV, a positive parity can also be proposed. Due to the nature of the low-lying neutron s. p. orbitals in the $N = 82$–126 shell, the bound states in ^{134}Sn can be populated solely via *ff* decays of ^{134}In (see Fig. 11).

A particular remark should be made about the 354-keV transition, which is confirmed in this work as following the β decay of ^{134}In [15]. Due to the lack of $\beta\gamma\gamma$ or $\gamma\gamma$ coincidence relations, its assignment to one of the daughter nuclei

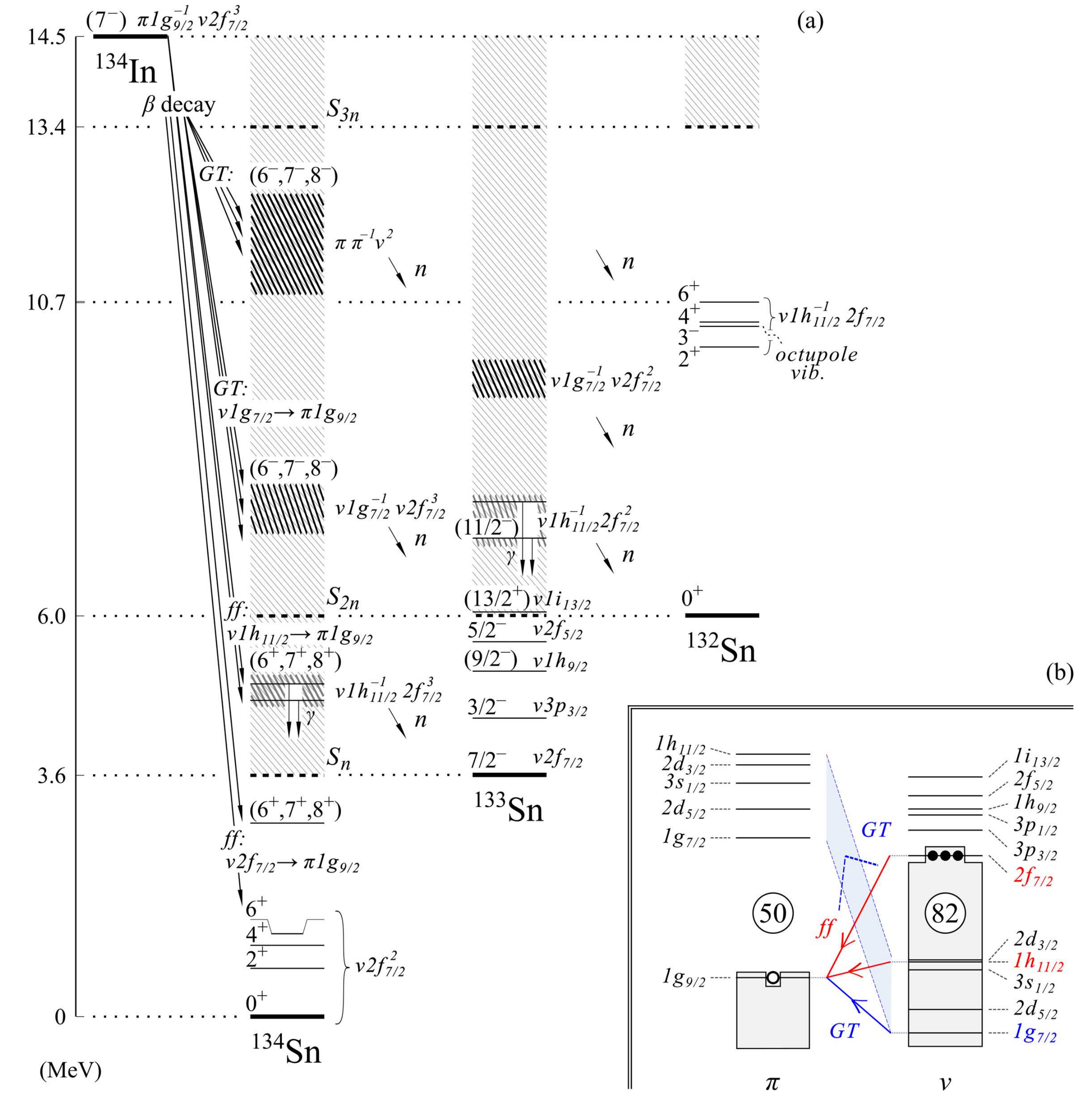

FIG. 11. (a) Schematic β-decay scheme of ^{134}In showing Gamow-Teller (GT) and first-forbidden (*ff*) transitions that populate neutron-unbound (gray striped areas) and bound states in the daughter nuclei. The expected excitation energies of unobserved states having core-excited configurations are indicated by black striped areas. Neutron-unbound states for which decay via γ-ray emission was observed are indicated. (b) Schematic representation of proton (π) and neutron (ν) orbitals relevant for the β decay of ^{134}In [61]. The ground-state configuration of the parent nucleus is schematically represented by circles indicating the location of valence neutrons (full circles) and proton hole (open circle) relative to the ^{132}Sn core.

is not possible. A state decaying directly to the ground state cannot be placed at such a low excitation energy in the level scheme of the $^{132–134}$Sn isotopes. In view of the enhanced contribution of electromagnetic transitions above S_n in ^{133}Sn and ^{134}Sn, one might consider the possibility that the 354-keV γ rays are emitted from a neutron-unbound state for which the centrifugal barrier hinders neutron emission. Once a γ ray has been emitted with the associated angular-momentum transfer, the level that has been fed could subsequently decay via neutron emission.

B. β decay of ^{135}In

The β-decay feeding pattern of the $N = 86$ ^{135}In is expected to be similar to that observed in the β decay of the $N = 84$ ^{133}In [22]. The ground state of ^{133}In has a $\pi 1g_{9/2}^{-1}\nu 2f_{7/2}^{2}$

configuration, while for the ground state of ^{135}In, an additional pair of neutrons occupies the $\nu 2f_{7/2}$ orbital. Based on systematics of the $Z = 49$ isotopes [59], a $9/2^+$ ground-state spin-parity assignment is expected for both ^{133}In and ^{135}In. For the ^{133}In nucleus, this spin value is supported by the observed β-decay feeding to levels in ^{133}Sn [22] with well-established spins and parities [13,19].

As discussed in the previous section for ^{134}In, the β decays of neutron-rich indium isotopes with $N > 82$ are dominated by the GT $\nu 1g_{7/2} \rightarrow \pi 1g_{9/2}$ transition populating states above S_{1n} in the daughter nuclei. Therefore, the ^{135}In β decay is also dominated by the βn-decay branches, as was observed in this work. The analogous state attributed to this GT decay was proposed in ^{133}Sn at an excitation energy of around 6 MeV [22]. The lowest-lying states populated via the $\nu 1g_{7/2} \rightarrow \pi 1g_{9/2}$ β decay can be expected in ^{135}Sn at comparable energies, being close to the S_{2n} of 5901(4) keV [27]. Based on the observations from the β decay of ^{134}In, other GT transitions involving deeply bound orbitals in the ^{132}Sn core also contribute, which enhances the $\beta 1n$- and $\beta 2n$-decay branches of ^{135}In.

While the states populated via the dominant GT decays of ^{135}In are mainly due to particle-hole excitations across the $N = 82$ shell gap, levels at low excitation energies in ^{135}Sn can be interpreted as excitations involving neutron orbitals in the $N = 82$–126 shell. In analogous β decay of the $(9/2^+)$ ^{133}In ground state, only two bound states in ^{133}Sn are populated: the $7/2^-$ $(\nu 2f_{7/2})$ ground state and the $(9/2^-)$ $(\nu 1h_{9/2})$ excited state [22]. Since the structure of the three valence-particles nucleus ^{135}Sn is more complex than the one valence-particle nucleus ^{133}Sn, more bound states can be populated via *ff* transitions in ^{135}Sn than in ^{133}Sn. If we make an analogy to the ^{133}In β decay [22], then the population of states arising from the $\nu 2f^3_{7/2}$ and $\nu 2f^2_{7/2}1h_{9/2}$ configurations in ^{135}Sn is expected in the ^{135}In β decay. Taking into account the most probable $(9/2^+)$ ground-state spin of ^{135}In, the *ff*-type β decay should favor the population of $7/2^-$, $9/2^-$, and $11/2^-$ states in ^{135}Sn. Therefore, the 950- and 1221-keV transitions observed in the ^{135}In β decay are assigned as deexciting states in ^{135}Sn with proposed spin-parity values of $7/2^-$, $9/2^-$, or $11/2^-$.

C. Comparison with shell-model calculations

1. ^{134}Sn

Shell-model predictions for ^{134}Sn are compared with the excited states observed in this nucleus in Fig. 12. The previously reported states in ^{134}Sn, belonging to the $\nu 2f^2_{7/2}$ multiplet and one corresponding to the $\nu 2f_{7/2}1h_{9/2}$ configuration, are well reproduced by available shell-model calculations.

The experimental information obtained in this work resulted in a significant expansion of the level scheme of ^{134}Sn, including seven new states, of which one is tentatively proposed. Four levels were placed in the range of 2–3 MeV, where calculations indicate the existence of members of the $\nu 2f_{7/2}3p_{3/2}$ and $\nu 2f_{7/2}1h_{9/2}$ multiplets [75,77,86,87]. The interpretation of levels at excitation energies around 5 MeV differs for the various calculations. These differences are mainly due to the chosen model space. The calculations presented in Ref. [75] [shown in Fig. 12(a)] do not include the $\nu 1i_{13/2}$ orbital in the model space, but they do include core excitations by considering the $\nu 1h_{11/2}$ and $\nu 2d_{3/2}$ orbitals below the $N = 82$ shell gap. Excited states predicted above 5 MeV belong to core-excited states with a dominant $\nu 2f^3_{7/2}h^{-1}_{11/2}$ configuration. These are out of the model spaces of Refs. [77,78,86,87], which adopt a neutron valence space consisting of orbitals above the $N = 82$ shell gap only. At excitation energies exceeding 3.2 MeV [78], 3.5 MeV [86], and 4 MeV [77], respectively, they predict states of negative parity that arise from particle excitations, belonging to the $\nu 2f_{7/2}1i_{13/2}$ configuration.

TABLE III. Comparison of predicted and experimental values of P_{1n} and P_{2n} for ^{134}In. Results of calculations using three successively improved approaches based on QRPA: QRPA-1 [68], QRPA-2 [70], and QRPA + HF [28,71] as well as based on RQRPA [7] and EDM [8,69] are presented. Data were taken from Ref. [65]. Predictions of the EDM model after applying the cutoff model (EDM$_{\mathrm{cutoff}}$) [8,69] are also presented.

Method	P_{1n} (%)	P_{2n} (%)
QRPA-1	0.60	99.4
QRPA-2	6.5	86.7
QRPA + HF	78	15
RHB + RQRPA	18.9	46.8
EDM	64.5	2.2
EDM$_{\mathrm{cutoff}}$	28	39
Experiment	89(3)	9(2)

Reduced transition probabilities for $E2$ transitions in ^{134}Sn were calculated from the measured lifetimes of the 2^+, 4^+, and 6^+ levels. Figure 13 shows the comparison of the determined values with those reported previously and with theoretical predictions. The obtained $B(E2; 2^+ \rightarrow 0^+) = 1.3^{+1.7}_{-0.5}$ W.u. is in agreement with the previously reported, more precise, $B(E2)$ value from the Coulomb excitation [60], which is well reproduced by the shell-model calculations. The experimental $B(E2; 4^+ \rightarrow 2^+) = 2.25(7)$ W.u., which was measured for the first time in this work, is not reproduced by any of the available calculations, which consistently predict a value of about 1.6 W.u., similar to the $B(E2; 2^+ \rightarrow 0^+)$ rate. In the case of the $6^+ \rightarrow 4^+$ transition, the precision of the new experimental result, $B(E2; 6^+ \rightarrow 4^+) = 0.870(13)$ W.u., is significantly improved compared with earlier results [16,24]. For this transition rate, agreement was obtained with various variants of the shell-model predictions (see Fig. 13).

If we review the experimental and predicted trends of $B(E2)$ values for successive transitions between members of the $\nu 2f^2_{7/2}$ multiplet in ^{134}Sn, we find that the calculations do not predict such an increase in $B(E2)$ for the $4^+ \rightarrow 2^+$ transition as it was observed. A similar trend, although more pronounced, occurs for $E2$ transitions connecting states belonging to the analogous multiplet in the ^{208}Pb region, $\nu 2g^2_{9/2}$ in ^{210}Pb [90,91].

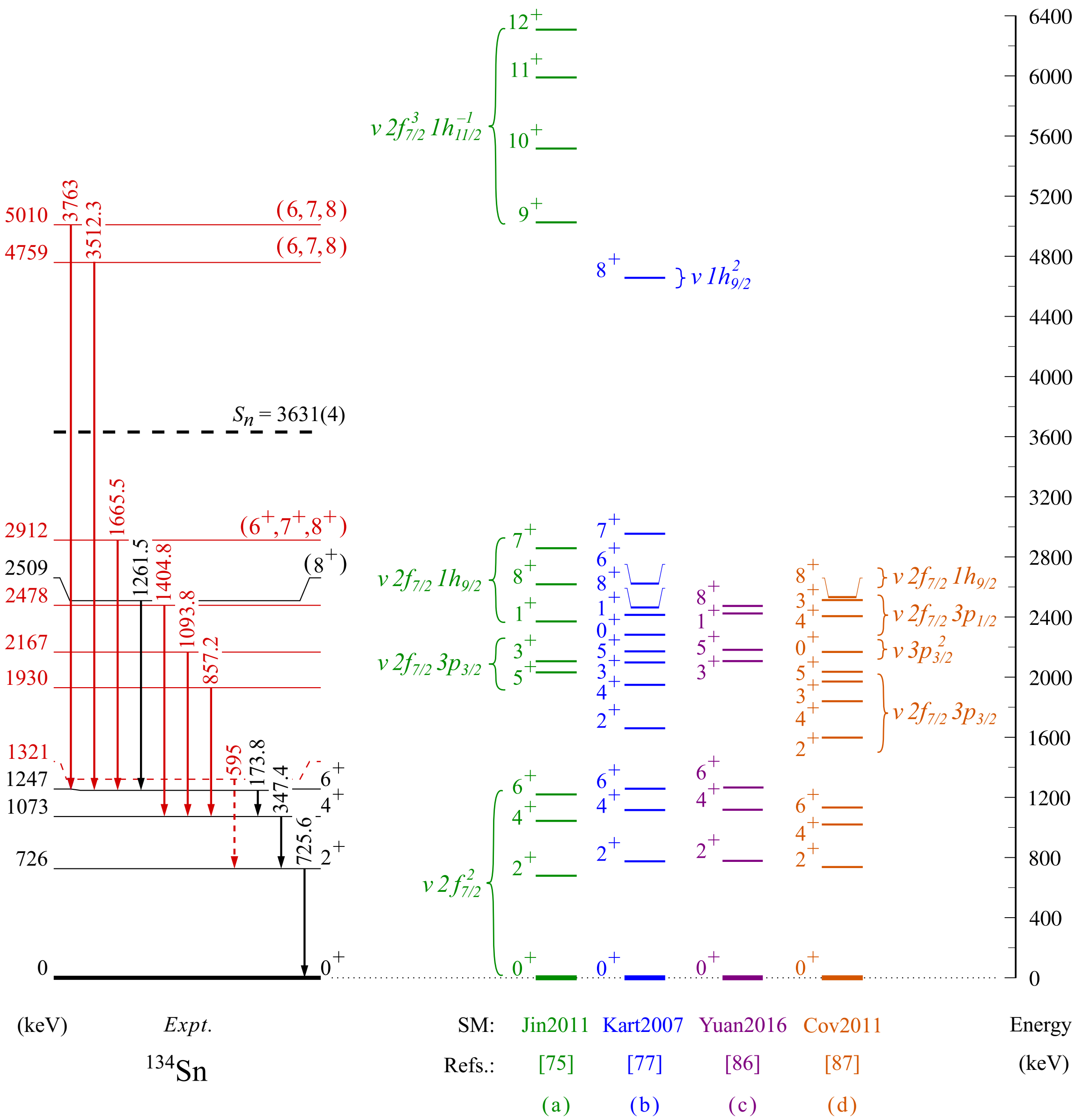

FIG. 12. Experimental (*Expt.*) level scheme of ^{134}Sn along with the results of the shell-model calculations (SM) (a) including neutron-core excitations, Jin2011 from Ref. [75], as well as employing ^{132}Sn as a closed core: (b) Kart2007 from Ref. [77], (c) Yuan2016 from Ref. [86], and (d) Cov2011 from Ref. [87]. The newly identified states are indicated in red. The level shown by the dashed line is proposed tentatively. The (8^+) state at 2509 keV [23] was not observed in this work. The experimental spin-parity assignments for previously known states in ^{134}Sn were taken from Refs. [16,23]. The S_n value for ^{134}Sn was taken from Ref. [27].

2. ^{135}Sn

Shell-model calculations for ^{135}Sn [77,78,86,88,92] provide guidance in the interpretation of the first experimental results on excited states for this nucleus. They predict a $7/2^-$ spin-parity for the ground state of ^{135}Sn, being a member of the $\nu 2f^3_{7/2}$ multiplet. This prediction is also supported by the systematics of excitation energies in the $N = 85$ isotones [93] as well as by the expected analogy to the ^{133}Sn nucleus, with a $7/2^-$ ground state [13].

The $5/2^-$ and $3/2^-$ levels are predicted to be the lowest-lying excited states in ^{135}Sn [77,78,86,88,92]. Given the expected $9/2^+$ ground-state spin-parity for ^{135}In, their population in the ^{135}In β decay is unlikely. States populated in ^{135}Sn via *ff* transitions most likely have spins and parities $7/2^-$, $9/2^-$, or $11/2^-$. Figure 14 displays the calculated excitation energies for low-lying $7/2^-$, $9/2^-$, and $11/2^-$ levels in ^{135}Sn. Shell-model calculations support the tentative assignment of the 950- and 1221-keV transitions to ^{135}Sn as ground-state transitions, since states with such spin values are expected in a comparable energy range [77,78,86,88,92]. Theoretical predictions tend to disagree when we consider levels at higher excitation energies in ^{135}Sn, arising from the $\nu 2f^3_{7/2}$, $2f^2_{7/2}\,3p_{3/2}$ and $\nu 2f^2_{7/2}\,1h_{9/2}$ configurations (see Fig. 14) [77,78,86,88,92].

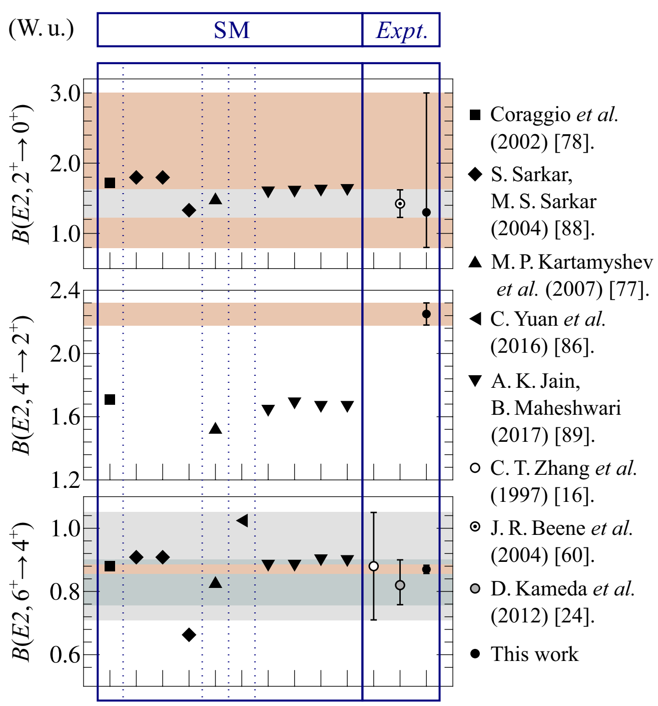

FIG. 13. Comparison of predicted (SM) and experimental (*Expt.*) reduced transition probabilities $B(E2)$ (in W.u.) for $E2$ transitions in ^{134}Sn. Presented data are taken from Refs. [16,24,60,77,78,86,88,89]. Uncertainties of the previously reported experimental results and the one obtained in this work are shown by the gray and orange areas, respectively.

V. SUMMARY AND CONCLUSIONS

We report on new γ-ray spectroscopy results from the ISOLDE facility at CERN on the β decay of the neutron-rich ^{134}In and ^{135}In nuclei, populating excited states in tin isotopes with $N \geqslant 82$. Due to the relatively simple structure of daughter nuclei, these β decays provide unique conditions for the simultaneous investigation of one- and two-neutron excitations as well as states formed by couplings of valence neutrons to excitations of the ^{132}Sn core.

The $\beta\gamma$- and $\beta 2n$-decay branches of ^{134}In have been observed for the first time. The β-decay scheme of ^{134}In was supplemented by thirteen transitions, of which three depopulate new levels in ^{134}Sn and two depopulate new levels in ^{133}Sn. Although the prevalent $\nu 1g_{7/2} \to \pi 1g_{9/2}$ GT transition feeds neutron-unbound states at excitation energies exceeding S_{2n} of ^{134}Sn, the ^{134}In β decay is dominated by $\beta 1n$ emission, with a probability of $P_{1n} = 89(3)\%$. Among the available global calculations of βn branching ratios, only the QRPA + HF [71] and EDM [8,69] models predict the predominance of this β-decay branch for ^{134}In. These two theoretical approaches take into account the competition between one- and multiple-neutron emission as well as γ-ray deexcitation in the decay of neutron-unbound states, which is not included in the other models considered.

A significant contribution of γ-ray emission from neutron-unbound states populated in the two daughter nuclei, ^{133}Sn and ^{134}Sn, at excitation energies exceeding S_{1n} by 1 MeV was observed in this work. The competition of γ-ray deexcitation with neutron emission well above S_{1n} can be explained by the weak overlap of the wave functions of states involved in βn emission. Neutron-unbound states emitting γ rays in ^{134}Sn are formed by couplings of valence neutrons to core excitations, while the low-lying levels in ^{133}Sn arise from one-particle excitations of valence neutron. In the energy range consistent with the predicted excitation energy of the $13/2^+$ state in ^{133}Sn, a 2434-keV transition was observed, which is proposed as a candidate for a γ ray depopulating the missing $\nu 1i_{13/2}$ s. p. state in ^{133}Sn.

Transitions following the β decay of ^{135}In were identified for the first time and the partial β-decay scheme of this nucleus was established. Three new transitions were assigned to ^{134}Sn based on $\beta\gamma\gamma$ coincidences. Two transitions were tentatively attributed to ^{135}Sn. Their placement in the level scheme of ^{135}Sn is supported by shell-model calculations. Several other γ rays were observed in the ^{135}In β decay

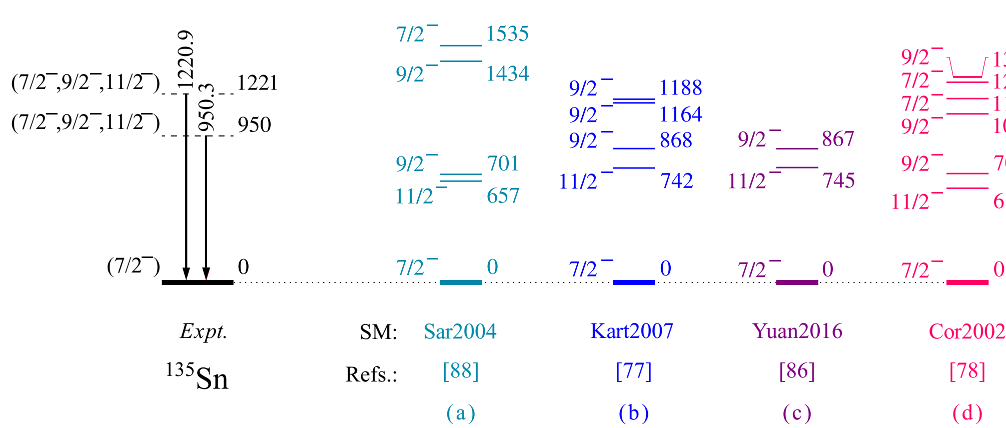

FIG. 14. Excited states in ^{135}Sn tentatively proposed in this work (*Expt.*). Calculated excitation energies (SM) for the $7/2^-$, $9/2^-$, and $11/2^-$ states in ^{135}Sn reported in (a) Sar2004 [88], (b) Kart2007 [77], (c) Yuan2016 [86], and (d) Cor2002 [78] are also presented. Excitation energies relative to the ^{135}Sn ground state are given in keV. The ground-state spin-parity assignment for ^{135}Sn, based on systematic trends in neighboring nuclei, was taken from Ref. [59].

but could not be assigned to a specific β-decay branch of the parent nucleus. Due to their low energies and lack of $\beta\gamma\gamma$ coincidence relations, they cannot be placed in the level scheme of any other daughter nuclei.

The level scheme of ^{134}Sn was supplemented in total by six new excited states, populated either through *ff* decays of ^{134}In or via $\beta 1n$ emission from neutron-unbound states in ^{135}Sn. Data from these two β decays also allowed us to determine the lifetimes of the previously known 2^+, 4^+, and 6^+ states in ^{134}Sn. Experimental excitation energies and reduced transition probabilities were compared with the shell-model calculations for ^{134}Sn. New levels appear at excitation energies for which existence of the $\nu 2f_{7/2}3p_{3/2}$ and $\nu 2f_{7/2}1h_{9/2}$ multiplets is predicted. Calculations including core excitations reproduce well the energies of the two neutron-unbound states identified in ^{134}Sn that are most likely populated in the *ff* $\nu 1h_{11/2} \rightarrow \pi 1g_{9/2}$ decays of ^{134}In.

ACKNOWLEDGMENTS

M.P.-S. acknowledges the funding support from the Polish National Science Center under Grants No. 2019/33/N/ST2/03023 and No. 2020/36/T/ST2/00547 (Doctoral scholarship ETIUDA). J.B. acknowledges support from the Universidad Complutense de Madrid under the Predoctoral Grant No. CT27/16-CT28/16. This work was partially funded by the Polish National Science Center under Grants No. 2020/39/B/ST2/02346, No. 2015/18/E/ST2/00217, and No. 2015/18/M/ST2/00523, by the Spanish government via Projects No. FPA2017-87568-P, No. RTI2018-09886 8-B-I00, No. PID2019-104390GB-I00, and No. PID2019-104714GB-C21, by the U.K. Science and Technology Facilities Council (STFC), the German BMBF under Contract No. 05P18PKCIA, by the Portuguese FCT under the Projects No. CERN/FIS-PAR/0005/2017, and No. CERN/FIS-TEC/0003/2019, and by the Romanian IFA Grant CERN/ISOLDE. The research leading to these results has received funding from the European Union's Horizon 2020 research and innovation programme under Grant Agreement No. 654002. M.Str. acknowledges the funding from the European Union's Horizon 2020 research and innovation program under Grant Agreement No. 771036 (ERC CoG MAIDEN). J.P. acknowledges support from the Academy of Finland (Finland) with Grant No. 307685. Work at the University of York was supported under STFC Grants No. ST/L005727/1 and No. ST/P003885/1.

[1] T. Otsuka, T. Suzuki, R. Fujimoto, H. Grawe, and Y. Akaishi, Phys. Rev. Lett. **95**, 232502 (2005).

[2] T. Otsuka, A. Gade, O. Sorlin, T. Suzuki, and Y. Utsuno, Rev. Mod. Phys. **92**, 015002 (2020).

[3] O. Sorlin and M.-G. Porquet, Prog. Part. Nucl. Phys. **61**, 602 (2008).

[4] Z. Q. Chen, Z. H. Li, H. Hua, H. Watanabe, C. X. Yuan, S. Q. Zhang, G. Lorusso, S. Nishimura, H. Baba, F. Browne, G. Benzoni, K. Y. Chae, F. C. L. Crespi, P. Doornenbal, N. Fukuda, G. Gey, R. Gernhauser, N. Inabe, T. Isobe, D. X. Jiang *et al.*, Phys. Rev. Lett. **122**, 212502 (2019).

[5] M. Birch, B. Singh, I. Dillmann, D. Abriola, T. D. Johnson, E. A. McCutchan, and A. A. Sonzogni, Nucl. Data Sheets **128**, 131 (2015).

[6] J. Liang, B. Singh, E. A. McCutchan, I. Dillmann, M. Birch, A. A. Sonzogni, X. Huang, M. Kang, J. Wang, G. Mukherjee, K. Banerjee, D. Abriola, A. Algora, A. A. Chen, T. D. Johnson, and K. Miernik, Nucl. Data Sheets **168**, 1 (2020).

[7] T. Marketin, L. Huther, and G. Martínez-Pinedo, Phys. Rev. C **93**, 025805 (2016).

[8] K. Miernik, Phys. Rev. C **90**, 054306 (2014).

[9] E. Margaret Burbidge, G. R. Burbidge, W. A. Fowler, and F. Hoyle, Rev. Mod. Phys. **29**, 547 (1957).

[10] K.-L. Kratz, B. Pfeiffer, O. Arndt, S. Hennrich, and A. Wöhr, Eur. Phys. J. A **25**, 633 (2005).

[11] B. Pfeiffer, K. L. Kratz, F. K. Thielemann, and W. B. Walters, Nucl. Phys. A **693**, 282 (2001).

[12] M. R. Mumpower, R. Surman, G. C. McLaughlin, and A. Aprahamian, Prog. Part. Nucl. Phys. **86**, 86 (2016).

[13] K. L. Jones, A. S. Adekola, D. W. Bardayan, J. C. Blackmon, K. Y. Chae, K. A. Chipps, J. A. Cizewski, L. Erikson, C. Harlin, R. Hatarik, R. Kapler, R. L. Kozub, J. F. Liang, R. Livesay, Z. Ma, B. H. Moazen, C. D. Nesaraja, F. M. Nunes, S. D. Pain, N. P. Patterson, D. Shapira *et al.*, Nature (London) **465**, 454 (2010).

[14] G. S. Simpson, G. Gey, A. Jungclaus, J. Taprogge, S. Nishimura, K. Sieja, P. Doornenbal, G. Lorusso, P.- A. Soderstrom, T. Sumikama, Z. Y. Xu, H. Baba, F. Browne, N. Fukuda, N. Inabe, T. Isobe, H. S. Jung, D. Kameda, G. D. Kim, Y.- K. Kim *et al.*, Phys. Rev. Lett. **113**, 132502 (2014).

[15] P. Hoff, P. Baumann, A. Huck, A. Knipper, G. Walter, G. Marguier, B. Fogelberg, A. Lindroth, H. Mach, M. Sanchez-Vega, R. B. E. Taylor, P. VanDuppen, A. Jokinen, M. Lindroos, M. Ramdhane, W. Kurcewicz, B. Jonson, G. Nyman, Y. Jading, K. L. Kratz *et al.* (ISOLDE Collaboration), Phys. Rev. Lett. **77**, 1020 (1996).

[16] C. T. Zhang, P. Bhattacharyya, P. J. Daly, R. Broda, Z. W. Grabowski, D. Nisius, I. Ahmad, M. P. Carpenter, T. Lauritsen, L. R. Morss, W. Urban, J. L. Durell, W. R. Phillips, M. J. Leddy, A. G. Smith, B. J. Varley, N. Schulz, E. Lubkiewicz, M. Bentaleb, and J. Blomqvist, Z. Phys. A: Hadrons Nucl. **358**, 9 (1997).

[17] P. Hoff, P. Baumann, A. Huck, A. Knipper, G. Walter, G. Marguier, B. Fogelberg, A. Lindroth, H. Mach, M. Sanchez-Vega, R. B. E. Taylor, P. van Duppen, A. Jokinen, M. Lindroos, M. Ramdhane, W. Kurcewicz, B. Jonson, G. Nyman, Y. Jading, K.-L. Kratz *et al.*, Hyperfine Interact. **129**, 141 (2000).

[18] K. L. Jones, F. M. Nunes, A. S. Adekola, D. W. Bardayan, J. C. Blackmon, K. Y. Chae, K. A. Chipps, J. A. Cizewski, L. Erikson, C. Harlin, R. Hatarik, R. Kapler, R. L. Kozub, J. F. Liang, R. Livesay, Z. Ma, B. Moazen, C. D Nesaraja, S. D. Pain, N. P. Patterson *et al.*, Phys. Rev. C **84**, 034601 (2011).

[19] J. M. Allmond, A. E. Stuchbery, J. R. Beene, A. Galindo-Uribarri, J. F. Liang, E. Padilla-Rodal, D. C. Radford, R. L. Varner, A. Ayres, J. C. Batchelder, A. Bey, C. R. Bingham, M. E. Howard, K. L. Jones, B. Manning, P. E. Mueller, C. D.

Nesaraja, S. D. Pain, W. A. Peters, A. Ratkiewicz *et al.*, Phys. Rev. Lett. **112**, 172701 (2014).

[20] V. Vaquero, A. Jungclaus, P. Doornenbal, K. Wimmer, A. Gargano, J. A. Tostevin, S. Chen, E. Nacher, E. Sahin, Y. Shiga, D. Steppenbeck, R. Taniuchi, Z. Y. Xu, T. Ando, H. Baba, F. L. Garrote, S. Franchoo, K. Hadynska-Klek, A. Kusoglu, J. Liu *et al.*, Phys. Rev. Lett. **118**, 202502 (2017).

[21] M. Piersa, A. Korgul, L. M. Fraile, J. Benito, E. Adamska, R. Álvarez, A. E. Barzakh, G. Benzoni, T. Berry, M. J. G. Borge, M. Carmona, K. Chrysalidis, G. Correia, C. Costache, T. Day Goodacre, D. V. Fedorov, V. N. Fedosseev, G. Fernáandez-Martínez, M. Fila, D. Galaviz *et al.*, Acta Phys. Pol., B **49**, 523 (2018).

[22] M. Piersa, A. Korgul, L. M. Fraile, J. Benito, E. Adamska, A. N. Andreyev, R. Álvarez-Rodríguez, A. E. Barzakh, G. Benzoni, T. Berry, M. J. G. Borge, M. Carmona, K. Chrysalidis, J. G. Correia, C. Costache, J. G. Cubiss, T. Day Goodacre, H. De Witte, D. V. Fedorov, V. N. Fedosseev *et al.* (IDS Collaboration), Phys. Rev. C **99**, 024304 (2019).

[23] A. Korgul, W. Urban, T. Rząca-Urban, M. Rejmund, J. L. Durell, M. J. Leddy, M. A. Jones, W. R. Phillips, A. G. Smith, B. J. Varley, N. Schulz, M. Bentaleb, E. Lubkiewicz, I. Ahmad, and L. R. Morss, Eur. Phys. J. A **7**, 167 (2000).

[24] D. Kameda, T. Kubo, T. Ohnishi, K. Kusaka, A. Yoshida, K. Yoshida, M. Ohtake, N. Fukuda, H. Takeda, K. Tanaka, N. Inabe, Y. Yanagisawa, Y. Gono, H. Watanabe, H. Otsu, H. Baba, T. Ichihara, Y. Yamaguchi, M. Takechi, S. Nishimura *et al.*, Phys. Rev. C **86**, 054319 (2012).

[25] R. Surman, M. Mumpower, and A. Aprahamian, JPS Conf. Proc. **6**, 010010 (2015).

[26] I. Dillmann, M. Hannawald, U. Köster, V. N. Fedoseyev, A. Wöhr, B. Pfeiffer, D. Fedorov, J. Shergur, L. Weissman, W. B. Walters, and K.-L. Kratz, Eur. Phys. J. A **13**, 281 (2002).

[27] M. Wang, W. J. Huang, F. G. Kondev, G. Audi, and S. Naimi, Chin. Phys. C **45**, 030003 (2021).

[28] M. R. Mumpower, T. Kawano, and P. Möller, Phys. Rev. C **94**, 064317 (2016).

[29] R. Yokoyama, R. Grzywacz, B. C. Rasco, N. Brewer, K. P. Rykaczewski, I. Dillmann, J. L. Tain, S. Nishimura *et al.*, Phys. Rev. C **100**, 031302(R) (2019).

[30] G. Lorusso, S. Nishimura, Z. Y. Xu, A. Jungclaus, Y. Shimizu, G. S. Simpson, P.-A. Söderström, H. Watanabe, F. Browne, P. Doornenbal, G. Gey, H. S. Jung, B. Meyer, T. Sumikama, J. Taprogge, Zs. Vajta, J. Wu, H. Baba, G. Benzoni, K. Y. Chae *et al.*, Phys. Rev. Lett. **114**, 192501 (2015).

[31] R. Catherall, W. Andreazza, M. Breitenfeldt, A. Dorsival, G. J. Focker, T. P. Gharsa, Giles T. J., J.-L. Grenard, and F. Locci, J. Phys. G **44**, 094002 (2017).

[32] A. Gottberg, T. M. Mendonca, R. Luis, J. P. Ramos, C. Seiffert, S. Cimmino, S. Marzari, B. Crepieux, V. Manea, R. N. Wolf, F. Wienholtz, S. Kreim, V. N. Fedosseev, B. A. Marsh, S. Rothe, P. Vaz, J. G. Marques, and T. Stora, Nucl. Instrum. Methods Phys. Res., Sect. B **336**, 143 (2014).

[33] V. Fedosseev, K. Chrysalidis, T. Day Goodacre, B. Marsh, S. Rothe, C. Seiffert, and K. Wendt, J. Phys. G **44**, 084006 (2017).

[34] IDS Collaboration, http://isolde-ids.web.cern.ch/isolde-ids.

[35] V. Vedia, M. Carmona-Gallardo, L. M. Fraile, H. Mach, and J. M. Udías, Nucl. Instrum. Methods Phys. Res., Sect. A **857**, 98 (2017).

[36] H. Mach, R. L. Gill, and M. Moszyński, Nucl. Instrum. Methods Phys. Res., Sect. A **280**, 49 (1989).

[37] M. Moszyński and H. Mach, Nucl. Instrum. Methods Phys. Res., Sect. A **277**, 407 (1989).

[38] L. M. Fraile, J. Phys. G **44**, 094004 (2017).

[39] http://www.nutaq.com.

[40] J. Benito, L. M. Fraile, A. Korgul, M. Piersa, E. Adamska, A. N. Andreyev, R. Álvarez-Rodríguez, A. E. Barzakh, G. Benzoni, T. Berry, M. J. G. Borge, M. Carmona, K. Chrysalidis, C. Costache, J. G. Cubiss, T. Day Goodacre, H. De Witte, D. V. Fedorov, V. N. Fedosseev, G. Fernández-Martínez *et al.* (IDS Collaboration), Phys. Rev. C **102**, 014328 (2020).

[41] R. Lică, G. Benzoni, A. I. Morales, M. J. G. Borge, L. M. Fraile, H. Mach, M. Madurga, C. Sotty, V. Vedia, H. De Witte, J. Benito, T. Berry, N. Blasi, A. Bracco, F. Camera, S. Ceruti, V. Charviakova, N. Cieplicka-Oryńczak, C. Costache, F. C. L. Crespi *et al.*, J. Phys. G **44**, 054002 (2017).

[42] J. Benito, Ph.D. thesis, Universidad Complutense de Madrid, 2020, https://eprints.ucm.es/id/eprint/65223/.

[43] J. Blomqvist, A. Kerek, and B. Fogelberg, Z. Phys. A: At. Nucl. (1975) **314**, 199 (1983).

[44] T. Siiskonen and H. Toivonen, Nucl. Instrum. Methods Phys. Res., Sect. A **540**, 403 (2005).

[45] I. Abt, A. Caldwell, K. Kröninger, J. Liu, X. Liu, and B. Majorovits, Eur. Phys. J. A **36**, 139 (2008).

[46] M. Anders, D. Trezzi, A. Bellini, M. Aliotta, D. Bemmerer, C. Broggini, A. Caciolli, H. Costantini, P. Corvisiero, T. Davinson, Z. Elekes, M. Erhard, A. Formicola, Zs. Fülöp, G. Gervino, A. Guglielmetti, C. Gustavino, Gy. Gyürky, M. Junker, A. Lemut, M. Marta, C. Mazzocchi *et al.*, Eur. Phys. J. A **49**, 28 (2013).

[47] J. Chao, Appl. Radiat. Isot. **44**, 605 (1993).

[48] M. Baginova, P. Vojtyla, and P. P. Povinec, Appl. Radiat. Isot. **166**, 109422 (2020).

[49] M. Stryjczyk, Y. Tsunoda, I. G. Darby, H. De Witte, J. Diriken, D. V. Fedorov, V. N. Fedosseev, L. M. Fraile, M. Huyse, U. Köster, B. A. Marsh, T. Otsuka, D. Pauwels, L. Popescu, D. Radulov, M. D. Seliverstov, A. M. Sjödin, P. Van den Bergh, P. Van Duppen, M. Venhart, W. B. Walters, and K. Wimmer, Phys. Rev. C **98**, 064326 (2018).

[50] A. Korgul, P. Bączyk, W. Urban, T. Rząca-Urban, A. G. Smith, and I. Ahmad, Phys. Rev. C **91**, 027303 (2015).

[51] W. Reviol, D. G. Sarantites, J. M. Elson, J. E. Kinnison, A. Gargano, S. Bottoni, R. V. F. Janssens, J. M. Allmond, A. D. Ayangeakaa, M. P. Carpenter, H. M. David, A. Galindo-Uribarri, N. Itaco, T. Lauritsen, E. Padilla-Rodal, and S. Zhu, Phys. Rev. C **94**, 034309 (2016).

[52] B. Fogelberg, M. Hellström, D. Jerrestam, H. Mach, J. Blomqvist, A. Kerek, L. O. Norlin, and J. P. Omtvedt, Phys. Rev. Lett. **73**, 2413 (1994).

[53] T. Kibédi, T. W. Burrows, M. B. Trzhaskovskaya, P. M. Davidson, and C. W. Nestor, Nucl. Instrum. Methods Phys. Res., Sect. A **589**, 202 (2008).

[54] B. Fogelberg, B. Ekström, L. Sihver, and G. Rudstam, Phys. Rev. C **41**, R1890(R) (1990).

[55] Yu. Khazov, A. A. Rodionov, S. Sakharov, and B. Singh, Nucl. Data Sheets **104**, 497 (2005).

[56] C. A. Stone, S. H. Faller, and W. B. Walters, Phys. Rev. C **39**, 1963 (1989).

[57] A. A. Sonzogni, Nucl. Data Sheets **103**, 1 (2004).

[58] A. K. Jain, B. Maheshwari, S. Garg, M. Patial, and B. Singh, Nucl. Data Sheets **128**, 1 (2015).

[59] F. G. Kondev, M. Wang, W. J. Huang, S. Naimi, and G. Audi, Chin. Phys. C **45**, 030001 (2021).

[60] J. R. Beene, R. L. Varner, C. Baktash, A. Galindo-Uribarri, C. J. Gross, J. Gomez del Campo, M. L. Halbert, P. A. Hausladen, Y. Larochelle, J. F. Liang, J. Mas, P. E. Mueller, E. Padilla-Rodal, D. C. Radford, D. Shapira, D. W. Stracener, J.-P. Urrego-Blanco, and C.-H. Yu, Nucl. Phys. A **746**, 471 (2004).
[61] H. Grawe, K. Langanke, and G. Martínez-Pinedo, Rep. Prog. Phys. **70**, 1525 (2007).
[62] A. Jungclaus, A. Gargano, H. Grawe, J. Taprogge, S. Nishimura, P. Doornenbal, G. Lorusso, Y. Shimizu, G. S. Simpson, P.-A. Söderström, T. Sumikama, Z. Y. Xu, H. Baba, F. Browne, N. Fukuda, R. Gernhäuser, G. Gey, N. Inabe, T. Isobe, H. S. Jung *et al.*, Phys. Rev. C **93**, 041301(R) (2016).
[63] V. H. Phong, G. Lorusso, T. Davinson, A. Estrade, O. Hall, J. Liu, K. Matsui, F. Montes, S. Nishimura, A. Boso, P. H. Regan, R. Shearman, Z. Y. Xu, J. Agramunt, J. M. Allmond, D. S. Ahn, A. Algora, H. Baba, N. T. Brewer, C. G. Bruno *et al.*, Phys. Rev. C **100**, 011302(R) (2019).
[64] I. N. Borzov, Phys. Rev. C **67**, 025802 (2003).
[65] IAEA CRP Database: https://www-nds.iaea.org/beta-delayed-neutron/database.html.
[66] R. Caballero-Folch, I. Dillmann, J. Agramunt, J. L. Taìn, A. Algora, J. Äyst ö, F. Calviño, L. Canete, G. Cortés, C. Domingo-Pardo, T. Eronen, E. Ganioglu, W. Gelletly, D. Gorelov, V. Guadilla, J. Hakala, A. Jokinen, A. Kankainen, V. Kolhinen, J. Koponen, M. Marta *et al.*, Phys. Rev. C **98**, 034310 (2018).
[67] B. Moon, C.-B. Moon, P.-A. Soderstrom, A. Odahara, R. Lozeva, B. Hong, F. Browne, H. S. Jung, P. Lee, C. S. Lee, A. Yagi, C. Yuan, S. Nishimura, P. Doornenbal, G. Lorusso, T. Sumikama, H. Watanabe, I. Kojouharov, T. Isobe, H. Baba *et al.*, Phys. Rev. C **95**, 044322 (2017).
[68] P. Möller, J. R. Nix, and K.-L. Kratz, At. Data Nucl. Data Tables **66**, 131 (1997).
[69] K. Miernik, Phys. Rev. C **88**, 041301(R) (2013).
[70] P. Möller, B. Pfeiffer, and K.-L. Kratz, Phys. Rev. C **67**, 055802 (2003).
[71] P. Möller, M. R. Mumpower, T. Kawano, and W. D. Myers, At. Data Nucl. Data Tables **125**, 1 (2019).
[72] A. Spyrou, S. N. Liddick, F. Naqvi, B. P. Crider, A. C. Dombos, D. L. Bleuel, B. A. Brown, A. Couture, L. Crespo Campo, M. Guttormsen, A. C. Larsen, R. Lewis, P. Möller, S. Mosby, M. R. Mumpower, G. Perdikakis, C. J. Prokop, T. Renstrøm, S. Siem, S. J. Quinn, and S. Valenta, Phys. Rev. Lett. **117**, 142701 (2016).
[73] E. Valencia, J. L. Tain, A. Algora, J. Agramunt, E. Estevez, M. D. Jordan, B. Rubio, S. Rice, P. Regan, W. Gelletly, Z. Podolyak, M. Bowry, P. Mason, G. F. Farrelly, A. Zakari-Issoufou, M. Fallot, A. Porta, V. M. Bui, J. Rissanen, T. Eronen *et al.*, Phys. Rev. C **95**, 024320 (2017).
[74] A. Gottardo, D. Verney, I. Deloncle, S. Péru, C. Delafosse, S. Roccia, I. Matea, C. Sotty, C. Andreoiu, C. Costache, M.-C. Delattre, A. Etilé, S. Franchoo, C. Gaulard, J. Guillot, F. Ibrahim, M. Lebois, M. MacCormick, N. Marginean, R. Marginean *et al.*, Phys. Lett. B **772**, 359 (2017).
[75] H. Jin, M. Hasegawa, S. Tazaki, K. Kaneko, and Y. Sun, Phys. Rev. C **84**, 044324 (2011).
[76] K. Whitmore, C. Andreoiu, F. H. Garcia, K. Ortner, J. D. Holt, T. Miyagi, G. C. Ball, N. Bernier, H. Bidaman, V. Bildstein, M. Bowry, D. S. Cross, M. R. Dunlop, R. Dunlop, A. B. Garnsworthy, P. E. Garrett, J. Henderson, J. Measures, B. Olaizola, J. Park *et al.*, Phys. Rev. C **102**, 024327 (2020).
[77] M. P. Kartamyshev, T. Engeland, M. Hjorth-Jensen, and E. Osnes, Phys. Rev. C **76**, 024313 (2007).
[78] L. Coraggio, A. Covello, A. Gargano, and N. Itaco, Phys. Rev. C **65**, 051306(R) (2002).
[79] C. Ellegaard, J. Kantele, and P. Vedelsby, Phys. Lett. B **25**, 512 (1967).
[80] J. Chen and F. G. Kondev, Nucl. Data Sheets **126**, 373 (2015).
[81] J. Blomqvist, in *Proceedings of the 4th International Conference on Nuclei Far from Stability*, *Helsingor, Denmark, 1981*, CERN Report No. 81-09 (CERN, Geneva, 1981), p. 536.
[82] M. Sanchez-Vega, B. Fogelberg, H. Mach, R. B. E. Taylor, A. Lindroth, and J. Blomqvist, Phys. Rev. Lett. **80**, 5504 (1998).
[83] M. Sanchez-Vega, B. Fogelberg, H. Mach, R. B. E. Taylor, A. Lindroth, J. Blomqvist, A. Covello, and A. Gargano, Phys. Rev. C **60**, 024303 (1999).
[84] L. Coraggio, A. Covello, A. Gargano, and N. Itaco, Phys. Rev. C **80**, 021305(R) (2009).
[85] B. Fogelberg, H. Gausemel, K. A. Mezilev, P. Hoff, H. Mach, M. Sanchez-Vega, A. Lindroth, E. Ramström, J. Genevey, J. A. Pinston, and M. Rejmund, Phys. Rev. C **70**, 034312 (2004).
[86] C. Yuan, Z. Liu, F. Xu, P. Walker, Z. Podolyák, C. Xu, Z. Ren, B. Ding, M. Liu, X. Y. Liu, H. S. Xu, Y. H. Zhang, X. H. Zhou, and W. Zuob, Phys. Lett. B **762**, 237 (2016).
[87] A. Covello, L. Coraggio, A. Gargano, and N. Itaco, J. Phys.: Conf. Ser. **267**, 012019 (2011).
[88] S. Sarkar and M. Saha Sarkar, Eur. Phys. J. A **21**, 61 (2004).
[89] A. K. Jain and B. Maheshwari, Phys. Scr. **92**, 074004 (2017).
[90] M. S. Basunia, Nucl. Data Sheets **121**, 561 (2014).
[91] R. Broda, Ł. W. Iskra, R. V. F. Janssens, B. A. Brown, B. Fornal, J. Wrzesiński, N. Cieplicka-Oryńczak, M. P. Carpenter, C. J. Chiara, C. R. Hoffman, F. G. Kondev, G. J. Lane, T. Lauritsen, Zs. Podolyák, D. Seweryniak, W. B. Walters, and S. Zhu, Phys. Rev. C **98**, 024324 (2018).
[92] L. Y. Jia, H. Zhang, and Y. M. Zhao, Phys. Rev. C **76**, 054305 (2007).
[93] W. Urban, W. R. Phillips, I. Ahmad, J. Rękawek, A. Korgul, T. Rząca-Urban, J. L. Durell, M. J. Leddy, A. G. Smith, B. J. Varley, N. Schulz, and L. R. Morss, Phys. Rev. C **66**, 044302 (2002).